Global phase-stable radiointerferometric systems

A. F. Dravskikh, D. V. Korol'kov, Yu. N. Parijskiĭ, A. A. Stotskiĭ, A. M. Finkel'steĭn, and P. A. Fridman

Special Astrophysical Observatory of the Academy of Sciences of the USSR, Pulkovo
Usp. Fiz. Nauk **135**, 587–636 (December 1981)

We discuss from a unitary standpoint the possibility of building a phase-stable interferometric system with very long baselines that operate around the clock with real-time data processing. The various problems involved in the realization of this idea are discussed: the methods of suppression of instrumental and tropospheric phase fluctuations, the methods for constructing two-dimensional images and determining the coordinates of radio sources with high angular resolution, and the problem of the optimal structure of the interferometric system. We review in detail the scientific problems from the various branches of natural science (astrophysics, cosmology, geophysics, geodynamics, astrometry, etc.) whose solution requires superhigh angular resolution.

PACS numbers: 07.60.Ly, 06.30.Bp, 95.75.Kk, 93.85. + q

CONTENTS

INTRODUCTION

Observational astronomy has always been characterized by striving to obtain high-quality images of celestial objects with maximally high angular resolution. The sensitivity of a radiotelescope is determined by its area, while according to Rayleigh's criterion its resolution is determined by its maximum dimension d (λ/d, where λ is the wavelength). Therefore, an evident path for attaining maximal resolution in the initial period consisted in building radiotelescopes of ever larger dimensions. However, owing to the finite rigidity of constructions, the dimensions of parabolic mirrors has a limit (apparently of the order of 100-150 m). Thus the resolving power of single mirrors hardly exceeds 0.5–1′ in the centimeter range of wavelengths.

Thus, we must draw on more subtle ideas to improve the resolving power of radioastronomical systems. In particular, the restrictions on rigidity of constructions can be overcome by using variable-profile antennas of the type of RATAN-600, which allow one to realize an angular resolution of the order of several seconds of angle.

However, the most fundamental step in the directions of increasing resolution was undertaken by M. Ryle, who introduced the idea of aperture synthesis into the practice of radioastronomy. The essence of this idea in the general case consists in employing a multielement radiointerferometer with variable baselines for constructing the images. The multiplicity of baselines of such a system that are successively realized in time allows one to synthesize a filled aperture with a dimension considerably exceeding the dimensions of a single element. The most refined systems of this type at present are the Cambridge 5-km interferometer (England), the radiotelescope at Westerbork (Netherlands), and the large antenna grod (VLA) in the USA. The re-

 0038-5670/81/120949-28$01.80 © 1982 American Institute of Physics

strictions on the limiting dimension of such systems are determined by the difficulties of phase stabilization in transmitting the signals at distances greater than several tens of kilometers. This situation restricts the limiting angular resolution of aperture-synthesis systems, which amounts to 0.1″ in the centimeter range, e.g., for the VLA.

A further increase in the distances between the elements of a radiointerferometer, and hence an increase in its resolving power, was made possible by an idea advanced in 1965 in the USSR,[1-3] and realized in Canada[4] and in the USA[5] in 1967. This involved an interferometer with independent recording of signals and with baselines up to the limit of $2R_\oplus$. It was proposed in the same year in the USSR to combine the radiotelescopes existing at that time into a single radiointerferometric network, thus creating a "global radiotelescope" with a large collecting surface.

This is the brief prehistory of the events of the last several years (1977–1979), when well-developed proposals have been advanced in the leading radioastronomical collectives of the USA,[6] Western Europe,[7] the USSR,[8] and Canada[9] on creating continuous-action, phase-stable radiointerferometric systems with very long baselines. These should constitute a new type of broad-profile physical instrument. Possessing a high current sensitivity and a superhigh angular resolution (down to 0.0001″), instruments of this type should serve as the basis for performing qualitatively new studies in the fields of fundamental physics, cosmology, astrophysics, radiophysics, geophysics, astrometry, celestial mechanics, and metrology.

While differing in details of ideology and of technical solutions, the projects[6-9] essentially amount to the very similar views of the astronomers of different countries on the future of observational radioastronomy, at least up to 2000. The reason for this rare unanimity in defining the prospects of radioastronomy is not fortuitous, and involves the positive and negative experience accumulated during the past decade in working with radiointerferometers with very long baselines (VLBIs). In order to present from a unitary standpoint the most important feature that unites the different projects, we shall employ the classification of the different generations of radiotelescopes that is defined in the folklore of the commission on radioastronomy MAC as the four variants of "domestic bliss in the community of radiotelescopes" (Fig. 1). If we examine this society from this standpoint, we must conclude that it has successfully passed through the first three stages, while the projects mentioned above assume a transition to the fourth "polygamous" stage. For this reason the project[8] has been names "Poligam".[1)]

The essence of the "polygamist ideology" consists in creating a synthetic area via a set of a definite number N of telescopes that will achieve the needed flux sensitivity of the system, and a synthetic diagram that will

[1)]The first phase of this project envisions the combination into a phase-stable network of a small number of large radiotelescopes.

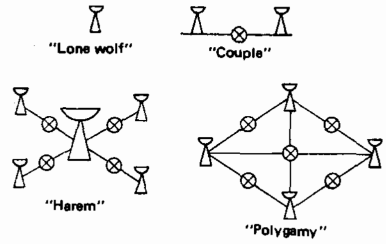

FIG. 1. The variants of "domestic bliss" in the community of radiotelescopes. The circle with an oblique cross ⊗ is a correlator.

achieve the needed angular resolution. Here the $N(N-1)/2$ baselines of such a system will facilitate the dense filling of the spatial-frequency plane.

This study is devoted to discussing the potentialities in principle of creating such a system with an angular resolution of 0.0001″, the methodological and technical problems that arise in realizing it, and its role in bringing unique observational information to natural science. We have tried to summarize the fundamental ideas of the national projects.[6-9] However, in spite of our trying to present objectively the essence of these projects, we have cast light most fully on the problems that have been studied in the Leningrad Branch of the Special Astrophysical Laboratory of the Academy of Sciences of the USSR.

1. INDEPENDENT INTERFEROMETRY

a) Interferometry with very long baselines. Fundamental observables

The block diagram in Fig. 2 illustrates the idea of an interferometer with a very long baseline. A high-stability generator-frequency standard exists at each station, whose signal is the reference for the heterodyne system and the electronic clocks. At a given particular

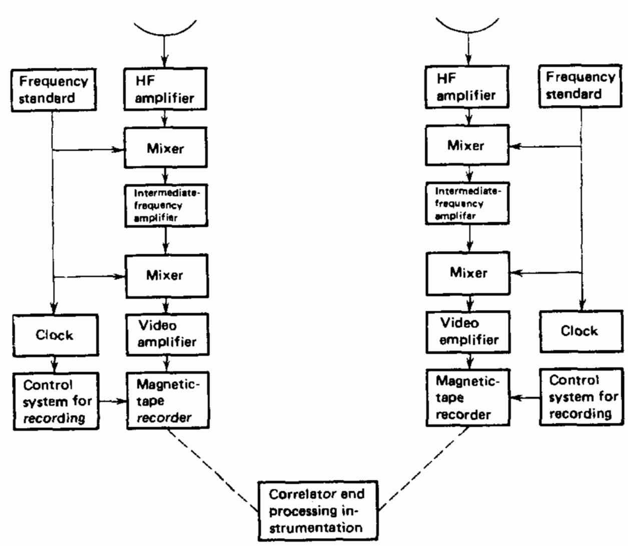

FIG. 2. Block diagram of the instrumentation of the stations of a VLBI.

instant of time (according to the clocks at the stations, which are correlated with the minimum possible error), the system is turned on for recording the signals from the radiotelescopes on magnetic tape. In contrast to a short-baseline interferometer with electric communication, where the intermediate frequency is sufficiently high, in a VLBI the spectrum of the noise signal is shifted into the region of video frequencies. Here the limiting frequency is determined by the capabilities of magnetic-tape recording. For the most refined tape recorders this amounts to 100 MHz. The recording continues from several minutes to half an hour. Then the magnetic tapes are taken to a computing center, where the recorded signals are subjected to correlation processing on universal computers or special processors. Thus the fundamental difference of VLBIs from traditional interferometers is the use of independent heterodyne systems, the recording of the signals on magnetic tape, and the processing of the signals after the observations ("off-line").

All the useful information on a source being observed with the interferometer is extracted by studying quantities quadratic in the field. In a correlation interferometer, in which the fields are multiplied together, this quantity is the response $R(t)$ to an extended source having the brightness distribution $I(\sigma)$ as smoothed by the diagram of the individual antenna (without taking into account the frequency characteristic of the receiver):

$$R(t)=V\exp\left[j\frac{2\pi}{\lambda}\rho\mathbf{k}(t)\right]. \tag{1}$$

Here

$$V=\int I(\sigma)\exp\left(j\frac{2\pi}{\lambda}\mathbf{w}\sigma\right) \tag{2}$$

is the visibility function, $\rho=\rho\mathbf{e}$ is the vector of the interferometer baseline, $\mathbf{k}$ is the unit direction vector to the source, and $\mathbf{w}=\mathbf{k}\times(\rho\times\mathbf{k})=\rho-(\mathbf{k}\cdot\rho)\,\mathbf{k}$ is the projection of the baseline vector on a plane perpendicular to the direction to the source (Fig. 3).

The two-element interferometer constitutes the elementary unit that measures the degree of spatial and temporal correlation of the fields from the source. We can see this feature of the interferometer even in treating the simple case of the response to a one-dimensional source having the angular dimension $\Delta\theta$ and the spectral flux density I_0 for an instrument having the passband Δf:

$$R(t)=I_0\cdot A^2(\theta)\left[\sin\left(\pi\frac{\rho}{c}\Delta f\cdot\cos\theta\right)\left(\pi\frac{\rho}{c}\Delta f\cos\theta\right)^{-1}\right]\times\sin\left(\frac{\pi\Delta\theta}{\lambda/\rho}\right)\left(\frac{\pi\Delta\theta}{\lambda/\rho}\right)^{-1}\cos\left(2\pi\frac{\rho}{\lambda}\cos\theta+\varphi_0\right). \tag{3}$$

Here θ is the angle between the directions of the baseline and the source, φ_0 is the initial phase of the interference signal, and λ is the wavelength. We see from (3) that the response is determined by the shape of the antenna diagram in terms of the power $A^2(\theta)$, by the shape of the frequency characteristic of the receiver, by the angular dimension of the source, and by the spatial frequency response $(\rho/\lambda)\,d\cos\theta/dt$. The first term having the form $\sin x/x$ indicates the possibility of loss of temporal coherence when the time lag $\tau=(\rho/c)\cos\theta$ becomes larger than $1/\Delta f$, while the second term of the same structure indicates the possibility of loss of spatial coherence when the angular dimension $\Delta\theta$ of the source becomes comparable with the lobe width $\Delta\theta \gtrsim \lambda/\rho$.

Equations (1) and (2) show that the visibility function is the Fourier transform of the radio brightness distribution of the source. Thus we can liken the radiointerferometer to a narrow-band spatial-frequency filter tuned to the frequency w/λ, so that the diurnal rotation of the Earth retunes the frequency of this filter (in the limiting case from 0 to ρ/λ).

The visibility function is determined by the two-dimensional radio brightness distribution $I(\sigma)$ and by the projection of the baseline on the plane perpendicular to the direction to the source (the uv plane). As one tracks the source, the diurnal rotation of the Earth causes the vector

$$\mathbf{w}=(u,v)=\rho\,(\cos\delta_b\sin(s-\alpha-\Lambda),\ \sin\delta_b\cos\delta-\cos\delta_b\sin\delta\cos(s-\alpha-\Lambda)),$$

to describe an ellipse in the uv plane:

$$\left(\frac{u}{a}\right)^2+\left(\frac{v-v_0}{b}\right)^2=1. \tag{4}$$

This ellipse has the parameters

$$a=\rho\cos\delta_b,\quad b=\rho\cos\delta_b\cdot\sin\delta,\quad v_0=\rho\sin\delta_b\cdot\cos\delta. \tag{5}$$

Here α, δ are the equatorial coordinates of the source ($s-\alpha=h$ is the hour angle of the source) δ_b and Λ are the declination and longitude of the baseline ($s-\Lambda=\alpha_b$ is the right ascension of the baseline). Therefore, if we measure the value of V in a large enough number of cells of the discrete uv plane (with a large enough number of projections of the baselines), then we can reconstruct $I(\sigma)$.

In problems involving positional measurements that are performed on point sources ($V=V_0$), the important information is conveyed by the time lag, which is determined by the path difference of the rays from the source to the antennas:

$$\tau=\frac{1}{c}\rho\cdot\mathbf{k}=\frac{1}{c}\rho_p\sin\delta+\frac{1}{c}\rho_e\cos\delta\cdot\cos(s-\alpha-\Lambda), \tag{6}$$

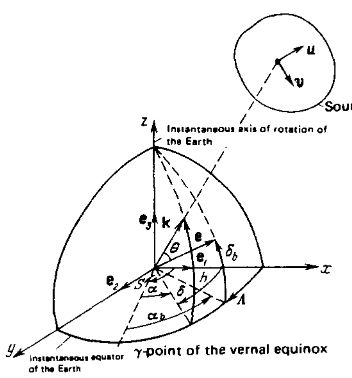

FIG. 3. Geometry of an interferometer in the equatorial system of coordinates. $\mathbf{e}=(\cos\delta_b\cos\Lambda,\ \cos\delta_b\sin\Lambda,\ \sin\delta_b)$ is the unit vector of the baseline; $\mathbf{k}=(\cos\delta\cos(s-\alpha),\ \cos\delta\sin(s-\alpha),\ \sin\delta)$ is the unit vector of the direction to the source.

TABLE I. Fundamental attainments of very-long-baseline radiointerferometry by the middle seventies.

Problems	Accuracy of determinations
Construction of models of images of radiosources	0.0005"
Determination of absolute coordinates	0.01"–0.05"
Determination of relative coordinates	0.001"
Determination of the length of a global baseline	4–6 cm
Worldwide time	0.07 ms
Coordinates of the pole	2–3 cm
Gravitational deflection of rays in the field of the Sun	1%
Determination of the position of astronauts on the Moon	1 m
Libration of the Moon	1"-selenocentric
Comparison of clocks	1 ns
Velocity of motion of a geostationary satellite	0.002 cm/s

Here $\rho_e = \rho\cos\delta_b$ and $\rho_p = \rho\sin\delta_b$ are the equatorial and polar projections of the baseline. Expressed in radians, this quantity amounts to the phase of the response to a point source $\varphi = (2\pi/\lambda)(\rho\cdot\mathbf{k})$. As the source moves through the interferometer diagram, since φ is a function of the time, an interference pattern arises of maxima alternating at the interference frequency:

$$F = \frac{\rho}{\varkappa}(\Omega\times\mathbf{e}\cdot\mathbf{k}) = -\frac{f\Omega}{c}\rho_e\cos\delta\cdot\sin(s-\alpha-\Lambda). \quad (7)$$

Here $\mathbf{\Omega} = \Omega\omega$ is the angular-velocity vector of the rotation of the Earth, and f is the frequency of the signal being received.

b) Difficulties of independent interferometry

The fundamental attainments in VLBI are summarized in Table I. If we look at these attainments from the most general standpoint, the most impressive ones are those in resolution. In the history of almost a half century of radioastronomy, the resolution has risen by a factor of more than 10^8 (the resolution of K. Jansky's first radiotelescope was about 30°), and by a factor of more than 10^5 in the past decade, owing to the introduction into practice of VLBI. However, doubts began to arise in the early seventies in the leading radioastronomical groups concerning the possibility of broad and effective application of VLBI. This situation stemmed from various circumstances. First, in the radiointerferometric systems being built *ad hoc*, the planning of even single experiments constitutes an extremely complex organizational problem, especially if the instruments forming the complex belong to different countries. In this connection, it has not yet been possible to create a "long-lived" specialized VLBI complex capable of solving complicated observational programs, especially of a "patrol" nature. Second, the processing of the data in interferometry with magnetic recording does not take place on a real time scale, and the results of even the primary data processing (obtaining the correlation functions) become known several months after the observations. Hence the possibilities of checking the obtained observational material prove highly limited. Finally, the most important defect of independent interferometry is that one cannot make phase measurements. Actually, the phase of the real interferometric response in (1) contains random phase shifts arising from the instability of the standards (φ_{app}) and the fluctuations of the electric thickness of the atmosphere (φ_{atm}):

$$\arg R = \frac{2\pi}{\lambda}(\mathbf{w}\cdot\sigma+\rho\cdot\mathbf{k}+c\tau_{app}+c\tau_{atm}) = \varphi(u,v)+\varphi_{geom}+\varphi_{app}+\varphi_{atm}. \quad (8)$$

This circumstance has far-reaching consequences for the effective use of the interferometer as an instrument for constructing images and determining the positions of cosmic sources.

First of all, measurement of only the amplitude of the visibility function $|V|$ allows only a certain representation of the structure and dimensions of the source being studied, and that only when some *a priori* information exists on a model for it (the "model fitting" procedure). Consequently the radio maps of sources become model-dependent.

Moreover, the random phase shifts limit the coherent recording time. This sharply decreases the limiting flux sensitivity of the system and does not allow one to study weak sources.

Finally, the lack of phase information allows one to determine the position of a source only within hundreds of lobes of the diagram, whereas modern radiotelescopes with filled apertures and phase-stable grids with small baselines determine the position of an object to hundredths of the diagram width.

Indeed, the root-mean-square errors in measuring the phase $\langle\varphi\rangle$, the time lag $\langle\tau\rangle$, and the interference frequency $\langle F\rangle$, which are associated with the additive noise of the apparatus, are:[2)]

$$\langle\varphi\rangle = \frac{1}{Q},\quad \langle\tau\rangle = \frac{\sqrt{3}}{\pi\Delta fQ},\quad \langle F\rangle = \frac{\sqrt{3}}{\pi TQ}. \quad (9)$$

Here the signal-to-noise ratio for an N-element interferometer is

$$Q = \frac{\pi}{32}\left(\frac{\sqrt{\Delta f\cdot T}}{kT_n}\right)d^2\sqrt{N(N-1)}\,F_{min}. \quad (10)$$

Also, d is the diameter of the antenna, F_{min} is the spectral flux density, Δf is the recording band, T is the time of recording, and T_n is the noise temperature of the system. Consequently, the errors in determining the angular position in measurements employing φ and τ are connected by the following relationship ($\langle\theta_\tau\rangle \approx c\langle\tau\rangle/\rho$, $\langle\theta_\varphi\rangle \approx \langle\varphi\rangle\lambda/2\pi\rho$):

$$\frac{\langle\theta_\tau\rangle}{\langle\theta_\varphi\rangle} \approx \frac{2\sqrt{3}f}{\Delta f}. \quad (11)$$

In the existing radiointerferometric systems the recording range is $\Delta f \lesssim 100$ MHz so that, for wavelengths $\lambda = 1-5$ cm, we have $\langle\theta_\tau\rangle/\langle\theta_\varphi\rangle \approx 1000-200$.

One can overcome all the above-listed defects of the existing radiointerferometers with very long baselines by rejecting the variant with independent recording of UHF signals and by connecting the radiotelescopes of the network via a geostationary retranslator satellite (Fig. 4). The vast digital communication bands (more than 1 GHz) enable one to increase sharply the sensitivity of the system by increasing the recording band and the number of elements of the network. The connecting of the heterodynes via the artificial satellite reduces the requirements on their long-term stability. This allows one to increase the time of coherent recording.[3)] All this taken together enables one to con-

[2)]To simplify the notation, everywhere below we shall denote the rms deviation of the quantity x by $\langle x\rangle$.

[3)]Interestingly, a very similar idea had been expressed in one of the pioneer studies on independent interferometry.[2]

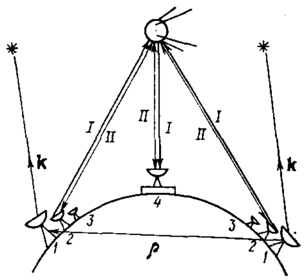

FIG. 4. Diagram of an interferometer with communication via a geostationary satellite. 1—radiotelescope, 2—communication antenna, 3—antenna for radiometric measurements of the eikonal, 4—receiving-transmitting antenna of the processing center, I—retranslation line of the main signal, II—transmission line of the heterodyne frequencies, time markers, and for communication between the stations.

struct the extensive net of reference objects needed for effective filtration of the phase noise of the troposphere. Finally, the transmission of the fundamental signals via a satellite with deposition and processing in a single center enables one to obtain information on the source in the real time scale ("on-line").

2. SCIENTIFIC PROBLEMS REQUIRING HIGH ANGULAR RESOLUTION

In planning large and expensive systems, one must specify clearly the set of scientific problems that this system can solve. Evidently the "lifetime" of the system, which one would like to maximize, is determined precisely by this set of problems.

In order for a system to be long-lived, it must possess the following qualities. To be universal, so as to furnish observational material for the maximal number of branches of natural science. To be extensible, which enables one steadily to increase its potential by adapting to new problems and objects, including those whose existence we cannot yet even suspect.[4)] To be oriented toward solving the problems of fundamental science for which "inflationary" tendencies are most weakly marked.

From the methodological standpoint, all the geometrical problems of observational astronomy can be classified into two large groups: a) problems involving construction of images of cosmic sources, and b) problems involving determination of positions of cosmic sources. This classification is historically fixed in the classification of observational astronomy into observational astrophysics and positional astronomy. The objective reason for the rise of this tradition primarily involves the fact that high-quality astrophysical and exact astrometric observations until recently could be performed only using different instruments, and as a rule, within the framework of different organizations.

In radiointerferometry, as a source passes through the synthesized diagram of the system, a signal appears at the output of the recording instrumentation that contains the necessary information both for constructing images and for determinations of position. Hence this tradition seems archaic now, and it is convenient only for continuing the presentation.

a) Problems involving construction of two-dimensional images of extended sources

If we speak in most general outline, the problems whose solution requires one to obtain high-quality images with a resolution from tenths of a second of arc to fractions of a millisecond of arc are:

a) on extragalactic sources—determination of the fundamental parameters of the Universe in the structure and dynamics of extragalactic sources, study of the processes of the formation, the dynamics, and energy production of quasars, spiral and Seyfert galaxies, and study of the global evolution of the extragalactic radiosources.

b) on galactic sources—study of the structure, dynamics, and energetics of the core of the Galaxy, of the regions of formation of stars and planetary systems, study of radio stars, and pulsars.

Multifrequency radio maps obtained in the continuum give a picture of the spatial distribution of relativistic electrons. When supplemented with polarization measurements, they allow one to reconstruct a picture of the magnetic fields and to estimate the electron density. Radio maps taken in radio lines yield very important information on the molecular and atomic composition (including the isotopic composition) of gas clouds, on their radial velocities, and on the structure of their magnetic fields. Finally, the study of the variability of radio images allows one to trace the dynamics of processes in the regions under study and to estimate their dimensions.

Let us proceed now to a more detailed description of certain problems whose solution requires one to obtain high-quality multifrequency images with a resolution of 0.1–0.001″ or better.

1. *Astrophysics.* a) Normal spiral, elliptical, and irregular galaxies, Seyfert galaxies, and quasars exhibit two types of structures—extended (1 kpc to 1 Mpc and greater) and compact (less than 1 kpc). As a rule, extended radio sources have a very complicated structure and contain two or more components separated by distances of up to millions of parsecs. The generally accepted model that enables interpretation to be made of the observed spectra, polarization, and structure of the extended sources is the synchrotron mechanism. According to this model the observed radiation is generated by the motion of relativistic electrons in magnetic fields, so that the radio spectrum reflects the energy distribution of the particles and the character of the magnetic field.

The central theoretical problem associated with the observations of extended sources is that of detecting the

---

[4)] In this regard it is pertinent to recall that in the late fifties, when the large paraboloids were being planned ($d > 50$ m), we were not yet acquainted with: pulsars, molecular masers, remnant radiation, quasars, and compact sources of synchrotron radiation in general.

primary energy source of these structures and of understanding the mechanism by which this energy (which constitutes a considerable fraction of the rest mass of the entire galaxy) is converted into relativistic particles and well-ordered magnetic fields so as to give rise to the observed energetics of a galaxy or quasar in time intervals at least of the order of 10^8 years.

Currently it is accepted to associate this primary source of the activity of galaxies and quasars with such compact and active structures as the cores. The compact cores of galaxies and quasars contain a considerable fraction of the energy of the entire source (e.g., the Galactic Center of dimension 200 astronomical units emits 10^{33} erg/s, of which about 25% arises from a core of dimension of the order of 10 astronomical units). The nature of the activity of the cores is still not clear, although a number of theories developed in varying degrees of detail has been advanced to explain this phenomenon, including some exotic ones: relativistic explosions of supernovas, rotational instability in the magnetosphere of spinars, accretion of interstellar gas by black holes, D-bodies, matter-antimatter annihilation, creation of matter, interaction of quarks, etc. The mechanisms of transport of particles from the cores to the extended components are equally poorly understood, and attempts to explain this process are varied: neutral and charged relativistic beams,[10,11] plasmon fluxes,[12] ejection of massive spinars,[13] etc.

In contrast to the extended sources, whose spectrum declines in the high-frequency region, the spectra of compact sources contain a peak in the low-frequency region (from dekameters to centimeters) involving the effect of synchrotron self-absorption (Fig. 5). Just like the extended sources, the compact sources having such spectra have a complicated, many-component structure and contain details with angular dimensions from 0.1″ to 0.001″ and smaller.[5)] To study such details, whose properties can cast light on the nature of the primary energy source, requires a resolution that cannot be attained with instruments with filled apertures nor with small-baseline interferometers. We note also that the measurement of the angular dimensions of compact sources at the dropoff frequency in the spectrum enables one to determine such an important characteristic as the magnitude of the magnetic field in the region being studied.[16]

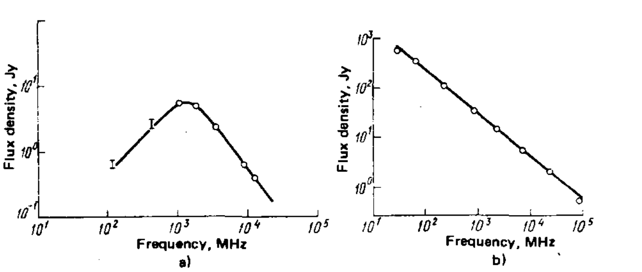

FIG. 5. Typical spectra of the compact source CTD 93 (a) and of the extended source 3C 123 (b).

The observations in very-long-baseline interferometers show that the compact details in Seyfert galaxies and quasars are characterized by variations of luminosity and structure. The discovered variations of intensity of radioemission (with periods from weeks to months) constitute a direct proof of periodic release of energy. This is important in principle for explaining the energetics of extended sources. This phenomenon is closely associated with the observed variation of the structure of compact sources, which is usually interpreted as periodic ejections of expanding clouds of charged relativistic particles that are initially optically thick. Therefore high-resolution observations are the main source of this information, which is extremely important in the problem of the energetics of galaxies and quasars.

Half of the compact sources with variable structure that have been studied at superhigh resolution have exhibited the remarkable phenomenon of superluminal dispersal of their components. In particular, the observations have shown that the quasars ZS273,[17,20,21,24,25] ZS279,[18-21,25] ZS345,[26] and the core of the Seyfert galaxy ZS120[22,23] contain details whose angular dimensions are smaller than or of the order of 0.0004″. The angular distance between these details is of the order of several milliseconds of arc, and it varies in secular fashion, so that the details are moving away from the center of mass with visible velocities of (2–15) c (Fig. 6). The nature of this phenomenon is not clear, though the number of models proposed to explain this effect is extremely large: motion of ultrarelativistic ejections,[28] successive flares of a series of unassociated sources ("Christmas tree"),[29] collision of two spherical shells,[19] motion of particles with a specially selected gas-density distribution[30] or a special geometry of the magnetic field,[31] flaring variations in the luminosity of the compact source,[32] a noncosmological nature of the red shift, etc. There are cogent grounds for thinking that this phenomenon is widespread. Thus an understanding of its physical nature can prove very important for explaining the mechanism of energy release of galaxies and quasars.

In studying the dynamics and energetics of objects of this type, it is extremely important to possess high-

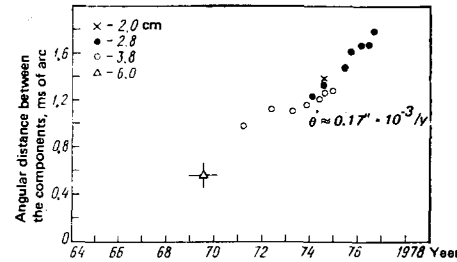

FIG. 6. Angular distance between the components of the quasar 3C 345 as a function of time.[27] For H_0 = 50 km/s Mpc, q_0 = 0.04, the apparent velocity of separation of the components $v_{\mathrm{exp}} = 4c$.

[5)]The extragalactic source having the smallest dimension of those observed by VLBI is a detail of the galaxy M87,[14] whose linear dimension is of the order of several light weeks. A detail has been found in the core of the spiral galaxy M81 with a linear dimension smaller than 1300 astronomical units.[15]

quality model-free images. This is particularly true if we recall that, in the studies cited above, the images of the sources were produced only from amplitude information. For this reason they employed various *a priori* models in constructing the images (two δ-functions, Gaussians, a ring, etc.) that might best represent the existing amplitude information. In this connection, the first attempts to explain the superluminal effect rejected simple two-component models with a flux constant in time, and adduced multicomponent models or models with a strong variability of components. Only recently has a series of VLBI experiments been performed[33-35] in which information on the "closure phase" was employed in addition to the amplitude information. These observations have shown that the previously observed effect is most likely model-independent. However, they also give a picture of the phenomenon only in general outline. In particular, the sign of the acceleration of the dispersing components is not yet known. A detailed study of this effect can be conducted only if the "model-fitting" procedure traditional for VLBI is replaced in constructing the images by inverse Fourier transformation of the visibility function, as is done in aperture-synthesis systems. Evidently this can be carried out only by using phase-stable multielement ("polygamous") systems with very long baselines.

A special role in understanding the nature of the primary energy source of the cores is played by the detailed study of the unique point source at the center of the Galaxy (the needed resolution is $\leq 0.001''$). In spite of the fact that the luminosity of the galactic center is smaller than that, e.g., of the spiral galaxy M81 by four orders of magnitude, and by 13 orders of magnitude smaller than that of the core of a typical quasar, nevertheless it is highly probable that it is a prototype of the active cores of galaxies and quasars.

As it appears now, the extended components of radiogalaxies and quasars are continuously being filled with relativistic particles generated by the cores. Although the connection between the compact cores and the extended components is not clear, yet there are observational data favoring the existence of such a connection. Often in radiogalaxies having axial symmetry (such as ZS236, Cygnus ZS111), the line joining the compact details has the same orientation as the extended radiosource does. This coincidence favors the idea of the existence of a unitary mechanism that governs the directionality of emission that acts on large space and time scales. The galaxy ZS111 is a good example of a situation in which the geometry of the compact core greatly resembles that of the extended component, though their linear dimensions differ by a factor of hundreds of thousands (Fig. 7).

In connection with the problem of the relation of the core to the extended components, we must mention another type of compact radioemission sources whose study requires a relatively high angular resolution, the so-called "hot spots", or regions in the extended components having an elevated brightness temperature. The resolution 0.1–0.01″ needed to study "hot spots" can be attained also in standard synthetic-aperture sys-

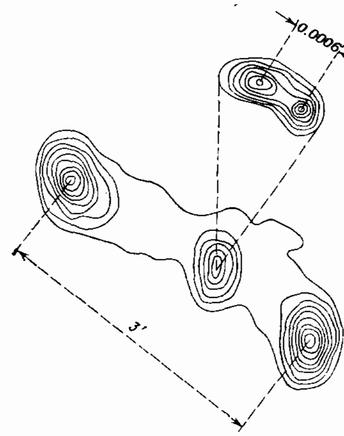

FIG. 7. Radio maps of the extended (3′) source 3C 111 (Westerbork) and of its compact core (VLBI).[1]

tems (particularly such as the VLA). However, the morphology of these regions can be effectively studied also in polygamous-type systems employing either long or relatively short baselines.

Thus a polygamous system enables one to construct detailed images of regions whose linear dimensions belong to the three characteristic ranges, and whose study is of fundamental interest for solving the problems of the activity of galaxies and quasars. First of all, there are the regions of dimensions smaller than 10 pc, which apparently are associated with the primary energy source. Further, there are the regions of dimensions 0.1–1 kpc, in which the energy transport from the core to the extended components takes place. Finally, there are the regions of dimensions of the order of 1 kpc, or "hot spots", from which the injection of particles into the extended components probably occurs. In this region, the polygamous system overlaps the synthetic-aperture systems in terms of problems and potentialities. In the regions of dimensions substantially larger than 1 kpc in which the particles diffuse and cool after injection into the extended components, the main observational information is furnished by synthetic-aperture systems and filled-aperture instruments.

b) The problem of stellar evolution is comparable in fundamentality and complexity with the problem of the energetics of extragalactic radio sources. The methods of very-long-baseline interferometry can prove to be the basic, and in a number of cases, the only means of obtaining observational information on the definite stages of stellar evolution.

Among the galactic sources bearing directly on this problem, the study of the maser sources (OH, H_2O, CH_3OH, and SiO) is of especial interest. All these sources have a very complex structure and contain a multitude of components with a broad spectrum of angular dimensions—from 0.1″ to 0.0001″ (the H_2O maser sources possess the smallest details). Maser sources can be divided into two classes. The first class includes the sources associated with compact H II regions. The latter amount to the ionized remnants of protostellar clouds surrounding O and B stars, so that studying them provides information on the early stages of stellar evolution. The second class contains the sources associated with cold stars that emit mainly in the infrared. Studying them provides information on the late stages of stellar evolution.

Among the most important questions involving maser sources that might be answered by high-resolution observations, we can note the following:[36] 1) what is the nature of the pumping of the cosmic masers? 2) are they saturated or unsaturated? 3) what is the geometry of the maser sources? 4) what is the nature of the variability of the profile of the lines and geometry of the cosmic masers? 5) are all the details of a maser source associated with a single star, or is each detail governed by its own star? 6) what is the connection between the maser sources of different types in a single region of the interstellar medium? 7) what is the connection between maser and compact radio sources?

An important role in the theory of stellar evolution can be played by observations of the fine structure of flaring stars and pulsars, which will enable us to determine more precisely the fundamental stages of stellar evolution, including the final stage. Total radioemission has been observed from many stellar objects: novas and supernovas, x-ray sources, double and flaring stars. Many radiostars show a variable intensity with periods of the order of one hour. Thus the dimensions of the radioemitting objects prove comparable with the dimensions of stars or with the distances between the components in double and multiple systems (≤ 10 astronomical units). This requires a high angular resolution for studying them. Unique VLBI observations show that sources on even smaller scales can exist. For example, a source has been resolved in Algol (β Persei) of dimensions 0.1 astronomical unit,[37] while observations of the known source Cygnus X-3[38,39] have shown that the dimension of the emitting region varies from 0.0013″ to 0.01″.

A new class of objects has appeared in recent years whose study requires high angular resolution. These are the objects of the type of SS 433, lying at the center of the remnants of supernovas and exhibiting vigorous changes in the position of the emission lines (as short as 0.3 s) and in brightness and structure (on the millisecond level). The interest in these objects is especially high because their evident genetic relation is being traced with the envelopes of supernovas, both in the x-ray ranges.

The most difficult problem is that of constructing an image of the magnetosphere of pulsars. Here one needs both high sensitivity and extreme resolution (as good as 0.0001″), as well as short wavelengths so as to suppress scattering effects. However, if one employs the reference-object method (see Sec. 4,a,1), one can expect to obtain an image of the pulsars closest to us averaged over many periods of the magnetosphere with a resolution higher than the dimension of the light cylinder.

2. *Cosmology*. a) The central theoretical problems of cosmology involve the elucidation of the nature of the initial state of the expanding universe and the mechanisms of formation of clusters of galaxies out of the primary perturbations of the hot plasma. The basic flow of observational radioastronomical information essential for solving these problems does not require a high angular resolution, and mainly involves measuring the temperature of the microwave remnant radiation. However, one can point out a class of problems for which it is important to obtain images with high angular resolution. These problems involve determining such cosmological parameters as the Hubble constant, the retardation factor, the curvature, etc.

In connection with these problems, we must first mention the surveys of the sky in a radiointerferometric regime for realizing such traditional tests as "the number of sources or angular dimension-flux density relationship". In principle, these tests allow one to determine the luminosity function, the evolution of the sources, and finally, the parameters of the cosmological model. For the sake of objectivity we note that the cosmological significance of these tests should not be exaggerated, since they depend more highly on the effects of evolution that on the cosmological parameters.

A more effective method of determining the cosmological parameters can involve using the effect of a gravitational lens.[41] As we know, the propagation of electromagnetic waves in a gravitational field can be treated from the standpoint of classical electrodynamics as the problem of propagation in a certain material medium whose effective refractive index depends on the gravitational potential. The latter is determined by the mass, spin, and the multipole moments of the object generating the gravitational field (gravitational lens). Rays of light grazing the gravitational lens on different sides can intersect it to give rise to annular or double structures of the source as seen through the lens, depending on whether the observer is on the focal axis or off it.[6)] The observed angular spacing between the images and the ratio of their intensities are determined in the simplest case of a Schwarzschild gravitational lens by its mass and by the mutual "source-lens-observer" geometry. As another independently observable quantity governed by the same parameters, there is the difference between the time intervals needed for the light rays from the two images to reach the observer while moving along the two paths of substantially different length. One can determine this quantity experimentally by intensity measurements (comparison of the brightness curves for variable sources or comparison of the two images for expanding objects), or by direct correlation of the fields from the two images of a point source. Together with a measurement of the red shift, all these observable quantities enable one in principle to determine the parameters of the gravitational lens, the distance to the source, and consequently, to refine the parameters of the cosmological model. As a whole, although this method depends on the model of the gravi-

[6)]A pair of quasars 0957 + 561 A, B has been found recently that lie at an angular spacing ~5.7″ from one another, and which have identical spectra. Quite likely they are two images of a single quasar having $z = 1.41$ generated by the gravitational lens of a galactic mass having $z = 0.39$.[42-44]

tational lens, it constitutes a method for directly determining extragalactic distances, in contrast to the traditional hierarchic method adopted in extragalactic astronomy.

We note that the study of the effect of gravitational focusing is of interest not only in connection with cosmological problematics, but also in connection with the new potentialities of interpretation of the observable features of the radio images of compact radio sources obtained at high angular resolution. In particular, perhaps, in some cases the point details in the cores of galaxies and quasars can prove to be images arising from the action of the lens effect, including lenses with masses of the order of $(10^3-10^4)\ M_\odot$.

b) Radiointerferometry with the longest possible baselines on Earth enables one to approach closely the Schwarzschild radius of large galactic black holes (if such exist) with masses of the order of $(10^6-10^8)\ M_\odot$. The study of such objects would make it possible to examine directly the physical processes in strong gravitational fields, i.e., in the regions where the description of the phenomenon of gravitation qualitatively differs in the different theories.[45] One of the first candidates for such a test can be the point source in the core of the Galaxy.

b) Problems involving measurement of positions of point sources

According to (6) and (7), the observables φ or τ and F have a simple geometric meaning: φ and τ determine the cosine of the angle between the direction to the source and the baseline, while F is the cosine of the angle between the perpendicular to the baseline lying in the plane of the instantaneous equator of the Earth and the vector **k**. Thus, from the standpoint of coordinate problems, the interferometer operates like a classical goniometric instrument. Just like the classical astrometric instruments, a very-long-baseline interferometer simultaneously defines the parameters characterizing the instrument itself while determining the coordinates of sources: the baseline vector, the time of desynchronization of the local scales of time, and the frequency difference of the local heterodynes. However, in contrast to the situation in classical positional astronomy, these "instrumental parameters" convey information full of interest.

To speak most generally, the most important problems that require coordinate measurements with the maximal resolution to solve them are:

a) the construction of an inertial system of coordinates whose reference objects are point details of the cores of galaxies and quasars, and the establishment of a connection between the optical and radio systems by using radio stars and optical pulsars,

b) the measurement of the parallaxes and proper motions of sources, at least within the Galaxy,

c) the measurement of large baselines and the study of the three-dimensional movements of points of the Earth's crust,

d) the study of the behavior of the angular-velocity vector of the rotation of the Earth in the inertial system of coordinates and of the motion of the pole in the body of the Earth.

1) *Astrometry*. a) The construction of an inertial system of coordinates (ISC) is traditionally viewed as the principal problem of astrometry. The ISC must possess the following basic properties[46]: 1) its definition must be maximally simple and accessible to a potential user, 2) its empirical definition must be based on the minimal number of nongeometrical assumptions, and it must be maximally independent of the tenets of special physical, geophysical, and astronomical theories, and 3) it must possess secular stability and must fully realize the potentialities of the existing technical means for coordinate measurements—to no poorer than a millisecond of arc.

Only VLBI measurements can create a system having the stated properties. First, they allow one to construct a system of relative positions of sources, including one independent of the mean equator and the instantaneous equator of the Earth. Second, they can make accessible extremely remote objects, most of which are immobile in image space at the millisecond level for hundreds of years. Third, among the ground-based means, only radiointerferometry can yield the required resolution—already the absolute coordinates of certain radio sources have been measured to an accuracy of 0.01″, which is almost an order of magnitude greater than the accuracy of the fundamental catalog FK 4.

Although the program of constructing an ISC is highly laborious, we must recall that the ISC is needed not *per se*, but only as a system that makes possible (primarily in a methodological sense) the solution of various astrophysical, geophysical, and geodynamic problems.[7)] In particular, in constructing the images of radio sources by the reference-object method, the ISC serves simply as a network of standard reference sources whose positions are known to high accuracy. Yet in the general case the ISC serves as a distinctive fundamental standard with which one can study the effects of various dynamic and phenomenological theories.

b) Even such primary coordinate information as the apparent relative positions of radio sources can have a direct application to fundamental science. As the most impressive example, it suffices to mention the verification with a record-setting 1% accuracy of one of the classical effects of the linear approximation of the general theory of relativity—the deflection of a light ray in the field of the Sun.[47] We note that our unshakable confidence in the correctness of the nonlinear approximation of the general theory of relativity is actually based

[7)]This is true not only as applied to VLBI methods. For example, a system of terrestrial coordinates constructed from laser and Doppler observations of a satellite can be autonomous if its accuracy does not exceed 5–10 m. At a higher accuracy, which is needed even in solving applied problems, a fundamental coordinate-time reference base such as a satellite is required.

only on a single high-accuracy test involving the processing of long series of observations, mainly optical, of one inner planet of the solar system—Mercury. For this reason any possible supplementary test of the nonlinear approximation of the general theory of relativity, particularly if not requiring gigantic expenditures of time, is highly prestigious. The unique goniometric potentialities of phase-stable very-long-baseline interferometry open up real prospects for performing such tests by measuring the relative angular distances between quasars, and also between quasars and planets and between planets[48] (in the latter two cases one must install "radio beacons" of the ALSEP type on the planets).

c) A qualitatively new possibility involving the high potentials of the system with respect to angular resolution is that of determining the distances to certain galactic sources by measuring the parallactic shifts of these sources against the background of reference extragalactic objects. At a resolution of 0.0001″, one can make parallax measurements up to distances of the order of 20 kpc. This possibility is very convenient for a direct test of the cosmological nature of the red shifts of certain quasars.

At distances up to 1 kpc, parallax measurements make possible distance determinations with an accuracy approaching 1%. At least 60 pulsars occur at this distance. Their distance measurements, supplemented with measurements of the Faraday rotation and the dispersion and absorption at 21-cm wavelength, yield information on the density and temperature of the electron gas and on the magnetic fields along the line of sight. This is important for understanding the physical conditions that exist in the interstellar medium.

In principle a possibility exists of measuring the parallactic shifts of extragalactic objects by employing the fact that the Earth is moving with respect to the remnant background with the velocity $v_{\odot} \approx 400$ km/s. A system with a resolution of 0.0001″ can detect a change in the position of a radio source lying at a distance up to 6 Mpc from the Earth relative to a more remote source via observations at a 10-year interval. However, if one includes space-borne elements in the ground-based radiointerferometric network, then with sufficiently long "Earth-Space" baselines, the possibility arises in principle of measuring distances in the Universe using the "curvature of the front".[49] The transport of two or three space radiotelescopes to great distances from the Earth (up to one astronomical unit) will bring all the objects in the Universe into the "near zone" of such an interferometer (the limiting distance at which such measurements can be made is $R = 2\pi\rho^2/\lambda \gtrsim 10^{28}$ cm $= 3000$ Mpc for $\rho \approx 10$ astronomical units and $\lambda \lesssim 10$ cm, which is comparable with the radius of curvature of the Universe).

d) Among the problems that require highly accurate positional measurements, we should mention the possible measurements of the proper motions of galactic radio sources. Measurement of the proper motions to an accuracy of 1 km/s with simultaneous measurement of the positions to an accuracy of 0.001″–0.0001″ allows one to localize the initial position of a source at distances of at least up to 1 kpc from observations for 5 years–0.5 year. As applied to pulsars, this implies that we might be able to localize the site of their formation and determine their ages. This is important in the theory of the evolution of neutron stars and supernova remnants.

A closely related problem that is important for astrophysics is the problem of seeking planets near radio-emitting stars from the perturbations of their positions by a heavy invisible companion. A planet of mass M_p lying at the distance r_{ps} from a star of mass M_s causes appreciable displacements of the position of the radio star against the background of immobile reference objects [the maximal angular displacement is $\sim (M_p/M_s)(r_{ps}/R)$]. In particular, a planet of mass $M_p/M_s \approx 10^{-3}$ lying at the distance $r_{ps} = 30$ astronomical units can be detected with a system with a resolution of 0.0001″ by measurements of the differential positions of a star lying at a distance up to $R = 300$ pc from the Earth.

In closing, let us make some remarks on the problem of the proper motions of the extragalactic radiosources that constitute the ISC. While the quasars lie at cosmological distances ($\gtrsim 10^{27}$ cm), most probably one can neglect their proper motions, which involve the peculiar velocity of the quasar as a whole. Actually, if we assume that these velocities are of the order of the galactic velocities ($\gtrsim 10^4$ km/s), the visible motions associated with these velocities will be of the order of 0.01 milliseconds of arc per year. Under these conditions, the ISC, which rests on these sources, will possess a millisecond secular stability. Thus no problems arise here such as are typical of optical astronomy. The situation is somewhat more peculiar when one employs sources that contain components moving at superluminal apparent velocities with respect to one another. The apparent proper motions of these details will be of the order of 0.001–0.0005″ per year, so that it is quite necessary to take these proper motions into account. Thus the qualitative cartography of these objects is not only of astrophysical interest, but it also plays the role of a type of utilization of the proper motions.

e) The placing in operation of an on-board optical telescope is being planned for the coming decade for solving astrometrical problems. It will be able to measure the relative angular distances between stars with millisecond accuracy (the "Hipparchus" project[50]). In order to interrelate the autonomous high-precision systems relying on optical and radiointerferometric observations, joint mass observations of stars in the optical and radio ranges are needed. Such observations in the radio range can be carried out in a "polygamous"-type system, since its high resolving power is directly associated with its high flux sensitivity.

2) *Geophysics, geodynamics, celestial mechanics.* a) The Earth constitutes an extremely complex thermodynamic system, in which the rheology of its material and the physics of interaction of the crust, mantle, and core are not fully understood. From the standpoint of such a central geophysical problem as studying the in-

ner structure of the Earth, an important role is played (in addition to the data from gravimetry and seismology) by radiointerferometric measurements of the magnitude and position of the angular-velocity vector $\mathbf{\Omega}$ of rotation of the Earth and of the variations of $\mathbf{\Omega}$ in time (precession and nutation). Various physical processes are responsible for the variations of $\mathbf{\Omega}$—the variation of the moment of inertia caused by the movement of the continents and earthquakes, dissipation of the energy of the solar and lunar tides, the circulation of the atmosphere, melting of ice, the change in the distribution of water masses in the ocean, crust-mantle interaction, etc. Each of these mechanisms, including those yet unknown, is typified by its own characteristic time scale—from 100 years to a half-day, and perhaps less. Therefore we need not only exact measurements of Ω (or of the length T of the day), but also measurements over as wide a spectal range as possible. A global system of photographic tubes makes it possible to determine T to an accuracy of 1 ms by averaging five-day cycles of observations. A radiointerferometric global network enables one to determine T to an accuracy of 50–10 μs. As is especially important, one can use it to study not only the low-frequency (3×10^{-10}–2×10^{-6} Hz) spectral components, but also the high-frequency components (10^{-5}–3×10^{-4} Hz) of the angular velocity of the rotation of the Earth, about which there has been as yet practically no observational information.

b) It is of great geophysical interest to study the free motion (in the Chandler frequency band with a period of ~14 months, and the free nutation with a period of the order of a day) and the forced movement of the pole in the body of the Earth, since this phenomenon is closely associated with the physics of interaction of the liquid core and the mantle. A system of zenith telescopes for international monitoring of the motion of the pole allows one to determine its coordinates with an interval precision up to 0.5 m (the absolute accuracy is somewhat poorer: 1–2 m) by averaging cycles of observations lasting a week. The potential resolution of a phase-stable radiointerferometric network can be as good as 1 cm with a substantially larger time resolution (up to an hour). One can attain comparable accuracy from Doppler (down to 10 cm) and laser (down to 1 cm) observations on an artificial satellite. However, radiointerferometric observations have the undoubted advantage over Doppler and laser observations that they are purely geometric in nature. Only near objects moving in the irregular and poorly studied gravitational field of the Earth are accessible to laser and Doppler observations. Here the problem of determining the coordinates of the pole is solved by dynamic means, which can lead to great difficulties in interpreting the results of exact determinations obtained by averaging series of at least a week in length.

c) A phase-stable system allows one to measure distances between points separated by thousands of kilometers (up to $2R_{\odot}$) to an accuracy of 1 cm, and to measure the three-dimensional motions of points of the Earth's crust in the system of stationary radio sources by tracing the time variations of the baseline vector.

The measurement of large baselines and their horizontal and vertical motions and rotations is of fundamental interest is solving problems of global tectonics of the lithospheric plates, and perhaps for predicting earthquakes in the seismically active regions. The radiointerferometric method of measuring relative distances between points is purely geometric. This distinguishes it favorably from the dynamic methods of Doppler and laser observations of an artificial satellite. In these methods the distances between points are calculated in terms of the barycentric coordinates of the points. This impedes the use of this information for solving problems of the global motions of points of the Earth's surface.

3) *Geodesics and applied problems.* a) We can treat the system of baselines of a multielement interferometer measured with high accuracy and verified by sources having well known positions as being a reference system of terrestrial coordinates. Any point of the Earth's surface can be referred to this autonomous system by using small transportable antennas tuned in to the system. The accuracy of such a reference (no worse than 10 cm) will be determined by the magnitude of the small baseline and the diameter of the transportable element.

b) The potentialities of radiointerferometric systems of relatively modest potential for navigation in near and far space have already been tested successfully,[51] so that the effectiveness of employing a "polygamous" system for these purposes arouses no doubt. The limits on the range in such a system will mainly be associated with the restricted power of the on-board source of the nomochromatic or noise signal.

c) Radiointerferometric coordinate measurements of any type allow one simultaneously to synchronize the local time scales to an accuracy up to fractions of a nanosecond. Thus the results of radiointerferometric measurements can serve not only fundamental science, but also serve as the basis for a coordinate-time reference service.

3. FACTORS COMPLICATING THE PERFORMANCE OF PHASE MEASUREMENTS

As we have already noted, two factors impede the performance of direct phase measurements in interferometry with independent heterodynes and very long baselines: instability of the frequency standards and the fluctuational properties of the Earth's troposphere. Both these factors, while having a different physical nature, act in the some way by introducing random phase shifts into the phase of the interference response in (8), which can lead to loss of coherence of signals.

a) Frequency standards. Time closure of stations

1) *Stability of frequency standards.* The basic function of the frequency standard in a radiointerferometry system with a very long baseline consists in producing a heterodyne signal. If the frequency difference of the heterodynes at the stations of the network were constant, while their baselines were stable, then no impediments would arise from the instrumental standpoint

TABLE II. Comparative characteristics of frequency standards.

Type of standard	Basic principle	Reproducibility	Stability			Volume, dm³	Mass, kg
			Short-term, < 1 s	Flicker, > 1 m	Drift per year		
H-maser	Active maser	10^{-12}	$5\cdot 10^{-13}$	$(2-5)\cdot 10^{-15}$	10^{-13}	1000	300
^{133}Cs	Passive, atom beam	Laboratory 10^{-13}	10^{-12}	10^{-14}	10^{-13}	2000	500
		Commerical 5×10^{-12}	$5\cdot 10^{-12}$	$5\cdot 10^{-14}$	$5\cdot 10^{-14}$	20	30
^{87}Rb	Passive, gas cell	High-quality 10^{-10}	$7\cdot 10^{-12}$	$4\cdot 10^{-13}$	10^{-10}	20	30
		Commerical 5×10^{-10}	10^{-11}	$5\cdot 10^{-13}$	10^{-9}	2	2

for obtaining the phases of the interference response. Actually the variances of the frequencies and phases remain small only for certain intervals of time, which determine the coherent-operation time of the generators taking part in the system.

Table II gives the parameters of the basic frequency standards that have been widely applied in radioastronomy, and in particular, in radiointerferometry. The rubidium standard has the poorest data with respect to accuracy and long-term stability. The drift of these standards is also poorer than for the other types. However, their advantages as compared with the other standards are their small dimensions, reliability, and cheapness. Since their short-term stability is no poorer than for the commercial cesium standards, they are usually employed as transportable standards. The cesium standards are the least widespread in radioastronomy. Their short-term stability is no better than for the rubidium standards, while their long-term stability is poorer than for the hydrogen standards.

Although the accuracy of the hydrogen standards is poorer than that of the cesium standards, their stability is the highest, they have the highest spectral purity. The stability of the hydrogen standards of the newest designs is as much as 5×10^{-15}, and we assume that it can be improved to 10^{-15}. This means that, for example, coherent recording is possible at a wavelength of 5 cm for more than 12 hours, so that standards at two stations will diverge within this time by less than a period. From the instrumental standpoint, this stability enables one to perform direct phase measurements. We note that hydrogen standards are expensive, stationary instruments, which are expediently applied as fundamental keepers of accurate time and frequency.

Figure 8 shows the data on the stability of the different standards applied in radioastronomy, and Fig. 9

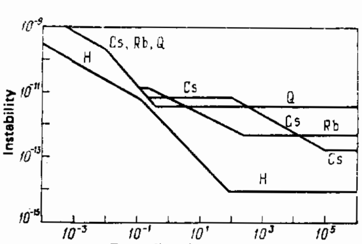

FIG. 8. Data on the stability of the fundamental atomic standards employed in radioastronomy.

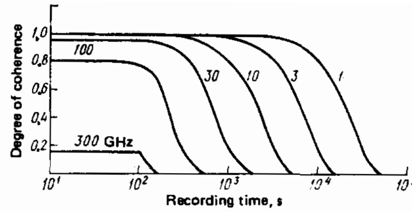

FIG. 9. Coherent recording time for a hydrogen standard.

shows the data on the time of coherent recording for a hydrogen standard.[40]

2) *Clock synchronization.* An electronic clock exists at each station of the network, and controls the recording process-start of recording and periodic insertion of time markers into the flow of data. The reference signal for the clock comes from the frequency standard. The readings of the local clocks at the different stations diverge for the following two reasons: a) existence of error in the initial setting of the clocks, and b) different running of the clocks owing to difference between the frequency standards.

Before starting recording, one must minimize the difference between the readings of the clocks at the stations. This is because, in the correlation processing of the signals, an error at the beginning of recording leads to prolonged searches for the correlation peak and substantially increases the time for processing. If the interval of time discretization is $\Delta t = 1/2\Delta f$, then we can consider the acceptable error in setting the clocks to be $\Delta\tau = 10\Delta t$. For a system having a recording band of $\Delta f = \pm 50$ MHz, we must have $\Delta\tau = +0.1$ μs.

The small dimensions of modern rubidium standards allows one to transport them along with the electronic clocks in the turned-on state in airplanes. At the beginning the standards and the clocks are checked at one of the stations, and then they are carried away to the stations of the system in the "hot" state. One uses the transportable standards to set more accurate standards, e.g., hydrogen standards, in frequency and epoch. After the completion of the observations, the transportable standards and clocks are brought together again to the central station, where a secondary comparison of frequencies and time is made. The differences obtained are employed for calculating the synchronization errors during the time interval between the two comparisons of the clocks. The accuracy of this method, which is widely applied in independent interferometry, can be less than 1 μs. However, the transportation of the clocks is a great inconvenience and is quite unacceptable in systems with real-time data processing.

From this standpoint, the method is considerably more convenient of comparing the clocks with signals from the LORAN-C system. The LORAN-C system is designed for navigational purposes,[53] but it can be employed to transmit exact time. There are eight networks of stations, each of which consists of a master and 2–4 slave stations. The stations emit series of radio pulses at the carrier frequency of 100 kHz synchronized with the UTC scale. The radio pulses can reach the receiver of a user by space or surface waves. Setting is done most accurately by the surface wave at distances up to 3000 km over the sea and 1500 km over dry land. There are two methods of setting time by using the LORAN-C system. The first employs the second pulses emitted by the stations in the intervals between the series. The accuracy of this method is not high—of the order of ±20 μs. The second method employs the fine structure of the radio pulses of the series. This allows an accuracy of setting of several tenths of a microsecond. Perhaps the only defect of this method of setting clocks is its inherent restriction in range.

The most natural method of synchronizing clocks for "polygamous"-type systems is retranslation of accurate-time signals via a geostationary artificial satellite,[54,55] which amounts to Einstein's classical method of synchronizing clocks. In this method the time signals ("time markers") at each station are transmitted to the retranslator satellite, and then are received at another station and again retranslated, whereupon they can be received at the initial station. Thus one measures the delay in retranslation. If one knows the delay and receives the time signals from the other stations, one can determine the discrepancy in the readings of the clocks. The accuracy of this method is of the order of 0.1 μs. This is quite sufficient for an effective search for correlation in broad-band reception. Further increase in accuracy of synchronization of clocks by using a satellite is not necessary, since the radio-interferometric system itself allows one to compare the scales to an accuracy of fractions of a nanosecond.

b) Effects of the propagation medium

When one has highly stable frequency standards and means of time closure of the stations via a satellite, the effect of the propagation medium (troposphere, ionosphere, interplanetary, and interstellar media) constitutes the fundamental factor impeding the formation of a phase-stable network. Tropospheric effects dominate in the centimeter range of wavelengths. Hence we shall treat them in special detail.

1) *Turbulent model of the troposphere.* The difference between the electrical thickness (eikonal) of the troposphere and its geometrical thickness at the zenith is as much as ~2 m. About 75% of this quantity is determined by the "dry" component of the air, and 25% mainly by water vapor (the "wet" component). Fluctuations in the temperature, pressure, and humidity arise from the turbulent mixing of the atmosphere, and lead to fluctuations in the eikonal.

As a convenient characteristic of the fluctuational properties of the eikonal, one can employ the spatial structure function $D_l(\rho) = \langle [l(x+\rho) - l(x)]^2 \rangle$. To construct this, one assumes a model of locally homogeneous isotropic turbulence.[56] In line with this, we can naturally consider three physically distinct ranges of variation of the structure function[57]:

$$D_l(\rho) = \begin{cases} C_l^2 \rho^{5/3}, & L_0 < \rho < L_1, \\ C_L^2 \rho^{2/3}, & L_1 < \rho < L_2, \\ C_L^2 L_2^{2/3}, & L_2 < \rho. \end{cases} \tag{12}$$

Here L_0 and L_1 are the internal and external scales of the isotropic three-dimensional turbulence, L_2 is the external scale of the two-dimensional turbulence, and C_l, C_L are the integral structure coefficients of the refractive index. In the approximation of geometric optics, the structure function of the phase $D_\varphi(\rho)$ differs from $D_l(\rho)$ only in the square of the wavenumber:

$$D_\varphi(\rho) = \left(\frac{2\pi}{\lambda}\right)^2 D_l(\rho) = k^2 D_l(\rho). \tag{13}$$

The persistence interval $L_0 < \rho < L_2$, in which the kinetic energy of the turbulent motion is considerably larger than the energy of dissipation and influx, is divided into two intervals of scale L_1. The latter scale coincides in order of magnitude with the effective thickness of the tropospheric layer $L \approx 6$ km. We can obtain the behavior in the persistence interval from geometric considerations. Actually, let two parallel rays of length L pass through the troposphere at the distance ρ from one another. If $\rho \ll L$, inhomogeneities of dimension ρ in a number $N = L/\rho$ are imposed on each ray. Then the phase difference that arises upon passing through a pair of such inhomogeneities is $\varphi_1 \approx k\rho\Delta n(\rho)$, where $\Delta n(\rho)$ is the difference between the refractive indices at points lying at the distance ρ. Consequently, the mean square of the phase difference is $\langle \varphi_1^2 \rangle \approx k^2\rho^2 D_n(\rho)$. Here the structure function of the refractive index obeys the Kolmogorov-Obukhov law $D_n(\rho) = C_n^2 \rho^{2/3}$, which is based on pure energy considerations. However, the total value of the mean square of the phase difference after passing through all N inhomogeneities will be: $D_\varphi(\rho) \approx k^2 L\rho D_n(\rho) \propto \rho^{5/3}$. However, if $\rho \gg L$, then each ray passes inside a single inhomogeneity of scale L, which determines the main contribution to the phase shift. Then we have $\varphi \approx kL\Delta n(\rho)$ and $\langle \varphi^2 \rangle = D_\varphi(\rho) \approx k^2 L^2 D_n(\rho) \propto \rho^{2/3}$, so that the structure function of the phase obeys the same "2/3 law" as the structure function of the refractive index.

The lower bound of the persistence interval L_0, which is determined by the rate of dissipation of the turbulence energy ε and by the kinematic viscosity ν: $L_0 = \nu^{3/4}\varepsilon^{-1/4}$, can be estimated rather reliably: $L_0 = 0.1$–1 cm.[8)] One can estimate with considerably less assurance the second boundary of the action of the 2/3 law, which is L_2. Apparently we should consider this bound to be the dimensions of the most powerful of the structures observed in the troposhere, the cyclonic storms, whose mean dimensions in the temperate latitudes vary in the range 2000–3000 km. When $\rho > L_2$ (the energy range in which "pumping" of energy mainly arises from the Sun), saturation of the structure function sets in.

The structure function in (12) represents satisfactorily the experimental results with the following choice of the structure coefficients and characteristic scales: $C_l = 1.7 \times 10^{-5}$ cm$^{1/6}$, $C_L = 0.013$ cm$^{2/3}$, $L_1 = 5.6$ km, and $L_2 = 3000$ km (Fig. 10).[58] Evidently the expression $(1/\sqrt{2})C_L L_2^{1/3} = 5.7$ cm determines the maximum rms val-

[8)]When $\rho < L_0$, we have $D_\varphi \propto \rho^2$. This is the region in which the energy pumped from the large-scale to the small-scale inhomogeneities is converted into heat owing to the viscosity (the viscous interval).

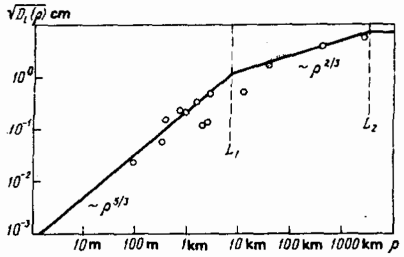

FIG. 10. Structure function of the eikonal of the troposphere. Circles—observations.

ue of the fluctuations of the electrical thickness of the troposphere at the zenith.

In order to prevent the troposphere from destroying the phase relations between signals arriving by different paths, we must have $\sqrt{D_l(\rho)} \ll \lambda/2\pi$. This relationship defines the minimum wavelength at which phase measurements remain possible. In particular, direct phase measurements on baselines $\rho \geq L_2$ are possible only starting in the decimeter range of wavelengths.

We can improve the situation substantially by supplementing the radioastronomical observations with special measurements of the eikonal at the stations of the system. One can take into account the "dry" component with an accuracy better than 1 cm by ground measurements of the temperature and the pressure. However, to determine the "wet" component, which is subject to variations, we can use the fact that there is an almost linear relationship between the brightness temperature of the atmosphere in the water-vapor lines and the eikonal. As calculations and individual experiments have implied,[64a,b] joint measurements of the meteorological parameters at the surface of the Earth and radiometric measurements near the resonance line of water (1.35 cm) enable one to determine the eikonal to an accuracy up to 1 cm at the zenith. There are estimates[64c] that show that, if one performs the radiometric measurements at several frequencies in the regions of the resonance lines of water (1.35 and 0.164 cm) and oxygen (0.5 cm), then one can reduce the accuracy of determining the eikonal at the zenith to about 1 mm. Thus, by combining the operation of the interferometer with synchronous measurements of the eikonal, one can correct a large part of the tropospheric phase shift.

2) *Tropospheric limitations in coordinate measurements.* If we assume that the additive noise of the apparatus is small, then the fluctuations of the electric thickness of the troposphere prove to be the most substantial factor limiting the accuracy of coordinate measurements. General considerations make it evident that one can diminish the tropospheric error in an angular measurement by using time accumulation. It seems at first glance that the effect of time accumulation should be quite considerable. Actually, if we introduce the time $t_\rho = \rho/v$ characteristic of the baseline ρ (v is the velocity of transport of the tropospheric inhomogeneities, or the wind velocity)[9], then the impression arises that one can make $N = T/t_\rho$ independent readings in a time $T \gg t_\rho$, and hence can diminish the tropospheric error of an instantaneous angular measurement $\langle\theta_0\rangle$ by a factor of $\sqrt{T/t}$: $\langle\theta\rangle = \langle\theta_0\rangle/\sqrt{T/t_\rho}$. However, if we adopt this viewpoint, then for phase measurements we cannot avoid the following paradoxical conclusion: In the persistence interval in the region of isotropic three-dimensional turbulence ($\rho < L_1$), the tropospheric error of angular measurements decreases with decreasing baseline of the instrument. Actually, according to (12), we have $\langle\theta_0\rangle \approx [D_l(\rho)]^{1/2}/\rho = C_l\rho^{-1/6}$. Hence we have $\langle\theta\rangle = C_l\rho^{1/3}/(Tv)^{1/2}$, so that $\langle\theta\rangle \to 0$ as $\rho \to 0$. The explanation of this paradox is that t_ρ does not determine the correlation interval in the general case, the latter always being larger than t_ρ when $\rho < L_2$. A decrease in $\langle\theta\rangle$ facilitates time filtration, which suppresses fine-scale inhomogeneities, and spatial filtration, which suppresses large-scale inhomogeneities. Therefore the character of the time averaging depends on the mutual relationship of T and t_ρ and the characteristic times $t_0 = L_0/v$, $t_1 = L_1/v$, and $t_2 = L_2/v$.

In the general case the variance of the difference in electric path lengths for an instrument of baseline ρ for a single session of duration T is[59,60]

$$D_l^T(\rho) = \frac{1}{T^2}\left[S\left(T + \frac{\rho}{v}\right) + S\left(\left|T - \frac{\rho}{v}\right|\right) - 2S\left(\frac{\rho}{v}\right) - 2S(T)\right]. \tag{14}$$

Here we have

$$S(x) = \int_0^x (x-t)\,D(t)\,dt.$$

Evidently we find

$$D_l^T(\rho) = \begin{cases} D(\rho) - 2S(T)\,T^{-2}, & \text{if} \quad t_\rho \gg T, \\ D(Tv)\left(\frac{\rho}{vT}\right)^2 - 2S\left(\frac{\rho}{v}\right)T^{-2}, & \text{if} \quad t_\rho \ll T. \end{cases} \tag{15}$$

Consequently, the tropospheric error in measuring the direction to a source in terms of the phase or the time lag will have the following asymptotic expressions:

$$\langle\theta\rangle \approx \begin{cases} \left.\begin{matrix} C_l/\rho^{1/6}, & L_0 < \rho < L_1, \\ C_L/\rho^{2/3}, & L_1 < \rho < L_2, \\ C_L L_2^{1/3}/\rho, & L_2 < \rho \end{matrix}\right], & t_\rho \gg T, \\ \left.\begin{matrix} C_l/(vT)^{1/6}, & t_0 < T < t_1, \\ C_L/(vT)^{2/3}, & t_1 < T < t_2 \\ C_L L_2^{1/3}/vT, & t_2 < T,\ \rho < L_2 \end{matrix}\right], & t_\rho \ll T. \end{cases} \tag{16}$$

Thus time averaging begins to exert an effect only when $T \gg t_\rho$, and then the averaging process works considerably more slowly than is implied by the naive theory (Fig. 11).

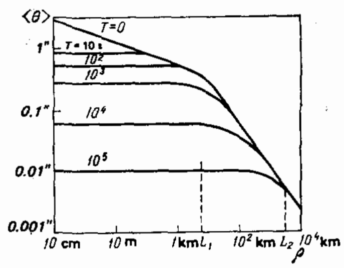

FIG. 11. Tropospheric limitations in phase measurements of coordinates.

[9] For the estimates below we have assumed $v = 10$ m/s, a value coinciding with the typical wind velocity in meteorological processes.

On baselines $\rho < L_1$, such as are typical of radiotelescopes with filled apertures and small-baseline radiointerferometers, one can attain a decrease in the fluctuational noise of the troposphere with long recording times. However, even in this case the troposphere limits the accuracy of angular measurement to hundredths of a second of arc. For baselines having dimensions in the region of action of two-dimensional turbulence, data accumulation diminishes the tropospheric limitations insignificantly, especially if we bear in mind that rigid instrumental restrictions on T exist here. Thus one can attain a further decrease in $\langle\theta\rangle$ only by going to baselines $\rho > L_2$. The data accumulation time plays practically no role in the energy range, and the decrease in $\langle\theta\rangle$ arises solely from the effect of saturating $D_l(\rho)$, which "clears up" the troposphere.[10)] This effect allows one to reduce the tropospheric error of a single angular measurement with large baselines to several milliseconds of arc. However, we must bear in mind that the actual limitations can be even more rigid, since the estimates given above pertain to the idealized case in which the source is observed at the zenith.

By using (14), we can easily find an expression for the variance of the rate of variation of the difference of electric path lengths[61]:

$$D_l^{\mathrm{T}}(\rho) = \frac{1}{T^2}\left[-D(\rho + vT) - D(|\rho - vT|) + 2D(\rho) + 2D(vT)\right]. \tag{17}$$

This allows us to estimate the tropospheric error in determining the direction to a source from the interference frequency (Fig. 12):

$$\langle\theta\rangle \approx \sqrt{D_l^T(\rho)}\,(\Omega\rho)^{-1} \approx \sqrt{2}\,\Omega^{-1}\begin{cases}\left.\begin{matrix} C\;{}^{5/6}/\rho T^{1/6}, & t_0 < T < t_1 \\ C_L v^{1/3}/\rho T^{2/3}, & t_1 < T < t_2 \\ C_L L_2^{1/3}/\rho T, & t_2 < T \end{matrix}\right], & t_\rho \gg T, \\ \left.\begin{matrix} C_l/\rho^{1/6} T, & L_0 < \rho < L_1 \\ C_L/\rho^{2/3} T, & L_1 < \rho < L_2 \\ C_L L_2^{1/3}/\rho T, & L_2 < \rho \end{matrix}\right], & t_\rho \ll T. \end{cases} \tag{18}$$

The spectrum of the fluctuations of F lies at considerably higher frequencies than the spectrum of fluctuations of the eikonal (Fig. 13). Therefore, time accumulation proves more effective in measurements employing

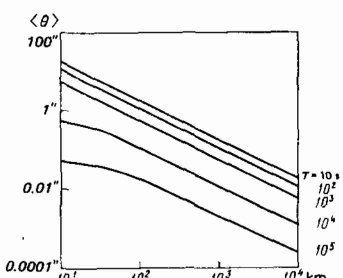

FIG. 12. Tropospheric limitations in frequency measurements of coordinates.

[10)]With baselines $\rho > L_2$, the regimes having $T > t_2$ are purely abstract in nature, and indirectly characterize the fact that we can treat the observations as statistically independent if the individual sessions are separated by time intervals greater than t_2.[60]

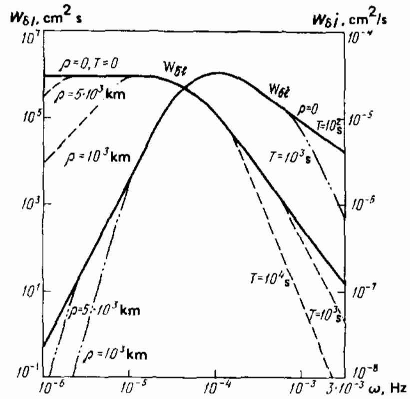

FIG. 13. Spectra of the fluctuations of the difference of electrical lengths $W_{\delta l}$ and of their velocities $W_{\delta \dot{l}}$.

the interference frequency than in measurements of φ or τ. However, even for considerable values of T, the tropospheric limitations in frequency measurements prove to be considerably more rigid because the rates of the variations of the eikonal have larger amplitudes. One can relax these limitations somewhat by taking into account the specifics of the procedure of coordinate measurements—a series of several readings during a relatively short interval of time and large intervals of time ΔT between series. In frequency measurements the individual series become statistically independent if $\Delta T > T$, so that in a daily cycle the tropospheric error can be reduced by a factor of $\sqrt{N}$, where N is the number of series.

Upon summarizing the situation as a whole, we must conclude that the fluctuational effects of the troposphere do not allow one in the centimeter wavelength range to measure directly the phase of an interference signal, and thus to realize the potential goniometric potentialities of a very-long-baseline radiointerferometer.

3) *Differential observations*. One can substantially reduce the effect of tropospheric noise by employing differential observations of sources (as applied to the problem of constructing images, this is the reference-object method[62]). The essence of this idea is that, while receiving the signal from a source 1 being studied, one observes simultaneously (or nearly so) another (reference) source 2 separated from it by the angular distance Ψ, and generates the phase differences $\Delta\varphi = \varphi_1 - \varphi_2$ as the observable quantities (Fig. 14).

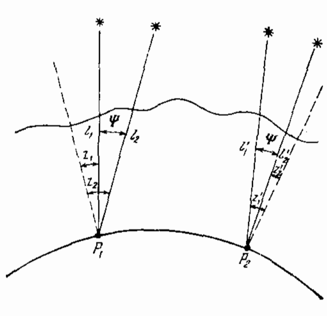

FIG. 14. On the idea of the reference-object method.

The application of this method is most effective when observing sources at the same zenith angles. In this case the geometric path lengths in the troposphere from the two sources to the antenna are the same ($l_1 = l_2$, $l_1' = l_2'$). As is evident from qualitative considerations, the tropospheric fluctuations caused by inhomogeneities having scales larger than $\rho_{eff} = L\Psi + v\,\Delta T$ ($\Psi \ll 1$, and ΔT is the time for shifting the antenna from the studied source to the reference source) will be subtracted in generating the differential phase. In this case the variance of the random phase shift $\Delta\varphi$ will be[63]:

$$\langle[\Delta\varphi]^2\rangle \approx \frac{k^2}{2}\left(\frac{1}{\cos^2 z_1}+\frac{1}{\cos^2 z_1'}\right) \times \begin{cases} \left.\begin{array}{ll} C_l^2\rho_{\text{eff}}^{5/3}, & Tv<\rho_{\text{eff}} \\ C_l^2\rho_{\text{eff}}^2/(vT)^{1/3}, & Tv>\rho_{\text{eff}} \end{array}\right], & T<t_1, \\ C_L^2\rho_{\text{eff}}^2/(vT)^{4/3}, & t_1<T<t_2. \end{cases} \tag{19}$$

Evidently the suppression of tropospheric effects will be more effective with decreasing Ψ. For baselines having $\rho > L_2$, the tropospheric limitations will not exceed a millisecond of arc even for $\Psi \sim 1$.

However, the situation in which the sources are being observed at the same z at both stations of a two-element interferometer is extremely rare, and is not realizable at all for a multielement system. However, in the case in which the sources lie at different zenith angles for baselines having $\rho \gtrsim L_2$, we have:

$$\langle[\Delta\varphi]^2\rangle = \frac{k^2}{2} C_L^2 L_2^{2/3}\left[\left(\frac{1}{\cos z_1}-\frac{1}{\cos z_2}\right)^2+\left(\frac{1}{\cos z_1'}-\frac{1}{\cos z_2'}\right)^2\right] \overset{\Psi\ll 1}{=} \frac{k^2}{2} C_L^2 L_2^{2/3}\left(\frac{\sin^2 z_1}{\cos^4 z_1}+\frac{\sin^2 z_1'}{\cos^4 z_1'}\right)\Psi^2. \tag{20}$$

The essential difference between the estimates of (20) and of (19) is that here the tropospheric phase shift is mainly governed by the inhomogeneities of largest dimensions, whereby the tropospheric limitations become more rigid. When $\lambda = 5$ cm, they lead to a shift in the differential phase $\langle\Delta\varphi\rangle > 180°$ even when $\Psi > 7°$ (Fig. 15).

Nevertheless, differential observations constitute the most effective method of reconstructing the phase of the interference response, both in coordinate measurements and in constructing images. The fact that phase reconstruction requires one to observe sources lying at small angular distances from one another leads to certain very strong requirements on the fluctuational flux sensitivity of the system. However, as will be shown (Sec. 5, b), one can satisfy these requirements with a certain number and dimension of the elements forming the system.

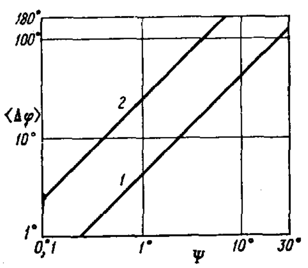

FIG. 15. Tropospheric shift in the differential phase $\Delta\varphi$ as a function of the angular distance Ψ between the sources. 1—the eikonal is measured; 2—the eikonal is not measured; $\rho = 3000$ km, $z_1 = 60°$, $z_1' \approx 33°$, $\lambda = 5$ cm.

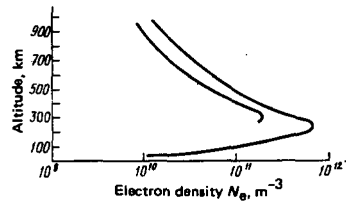

FIG. 16. Electron profiles of the ionosphere.

Differential measurements can be especially effective if we supplement them with special measurements of the eikonal at the stations of the system, and thus partially correct the tropospheric differential phase shift (Fig. 15).

4) *The ionosphere, interplanetary and interstellar media.* In contrast to the troposphere, the ionosphere amounts to a frequency-dependent medium in which the phase velocity of propagation of a wave is always larger than the velocity of light. Accordingly the phase shift from the ionosphere is opposite in sign to the tropospheric shift, and it depends on the frequency of the incident wave ($\propto f^{-2}$), on the electron density N_e, and on the magnitude of the Earth's magnetic field. The electron density distribution has a shape close to that shown in Fig. 16,[65] and it reaches a maximum at altitudes of 200–300 km. The profiles can be obtained for the lower layers of the ionosphere with probes or with microwave probing, and for the upper layers from the Faraday rotation of the signals from artificial satellites. For frequencies above 5 GHz, the ionospheric contribution is small in comparison with the tropospheric contribution, while it dominates for frequencies below 1 GHz. At the frequency $f = 1$ GHz it amounts to 10–20 m at the zenith (Fig. 17). This regular component of the ionospheric shift can be precalculated well with relatively infrequent measurements of N_e. At frequencies above 5 GHz the residual uncertainty will amount to less than 5–10 cm. This is a rather considerable magnitude for systems with high angular resolution. However, since the characteristic time of variation of N_e, including that involving turbulent movements, is about 0.5 hour (the characteristic scale of the inhomogeneities is ~400 km), the application of difference methods for diminishing the contribution from ionospheric refraction is no less effective than in the case of the neutral trop-

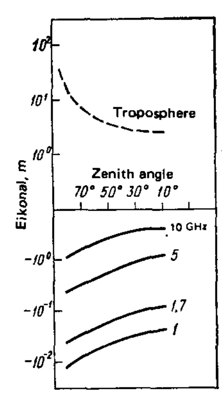

FIG. 17. Eikonal of the ionosphere for a particular station.

osphere. The effect of the ionosphere can be practically completely suppressed by employing multifrequency observations. This method is being successfully employed, for example, in the satellite navigational system "Navstar".

The interplanetary medium is highly inhomogeneous, and the fluctuations of its parameters extend from scales of 10 km to 1 astronomical unit, while the structure function of the eikonal is apparently a power function.[66] The fundamental scale of the turbulence is 10^6 km, while the corresponding characteristic time $t=4\times10^5$ s coincides with the time that it takes the solar wind to reach the orbit of the Earth. The latter implies that one can easily suppress the effect of the interplanetary medium by differential measurements.

The interstellar medium is as yet poorly studied. However, observation of scintillation of radio sources shows that the phase shift over distances of the scale of the source is much smaller than the period for wavelengths $\lambda \leq 10$ cm, even in the plane of the Galaxy.

4. METHODS OF PRODUCING IMAGES AND DETERMINING COORDINATES

a) Construction of two-dimensional images of extended sources

As we have already noted, the measurement of the amplitude $|V|$ of the visibility function enables one to obtain only model maps of sources. In order to obtain images by Fourier transformation of the visibility function in a situation in which $|V|$ is well known, while the phase contains random instrumental and tropospheric shifts, three methods have been proposed: a) the reference-object method,[61,67] b) the "closure phase" method,[68,69] and c) the multifrequency method.[67,70] All these methods amount to methods of phase comparison, since the phase of the signal for the source being studied is compared with the phase of the signal for another source whose radio brightness distribution is known, or with the phase of the signal from the same source obtained at another spatial frequency or at another wavelength. The possibility of constructing images by the cited methods involves the feature of radiointerferometry that the stages of generating the complex spectrum of spatial frequencies and constructing the image proper are separated in it. Therefore one can intervene in the process of image construction in the first stage by performing phase correction immediately before the Fourier transformation procedure.

1) *Reference-object method.* In this method the phase of the signal from the source being studied ($\arg R_1$) is compared with that ($\arg R_2$) of the reference source, whose structure is known. If the reference source is a point source, then we have $\varphi_2(u,v)=0$, and the difference phase is

$$\arg R_1-\arg R_2=\varphi_1(u,v)+\frac{2\pi}{\lambda}\rho(\mathbf{k}_1-\mathbf{k}_2)+\Delta\varphi_{\text{app}}+\Delta\varphi_{\text{atm}}. \quad (21)$$

Here $\Delta\varphi_{\text{app}}$ and $\Delta\varphi_{\text{atm}}$ are the residual phase shifts of apparatus and atmospheric origin. As we showed in Secs. 3, a, 1 and 3, b, 1, these shifts can amount to small fractions of the period if one employs hydrogen standards and generates the differential phase during a sufficiently short interval of time, and also if both sources lie at a sufficiently small angular separation Ψ. Thus the sought phase $\varphi_1(u,v)$ can be determined to the accuracy of the constant term $\Delta\varphi_{\text{geom}}$. According to (6), the expression for the latter in equatorial coordinates has the form

$$\Delta\varphi_{\text{geom}}=\frac{2\pi}{\lambda}\rho_p(\sin\delta_1-\sin\delta_2)+\frac{2\pi}{\lambda}\rho_e[\cos\delta_1\cos(\Omega t+\alpha_b^0-\alpha_1)-\cos\delta_2\cos(\Omega t+\alpha_b^0-\alpha_2)]. \quad (22)$$

Here α_b^0 is the right ascension of the baseline at the instant $t=0$.

Consequently the sought radio brightness distribution will be

$$I(\sigma)\propto {}^2F\left(\frac{R_1}{R_2}\right). \quad (23)$$

Here ${}^2F$ is a two-dimensional Fourier transformation.

In precalculating $\Delta\varphi_{\text{geom}}$, we must have $\langle\Delta\dot{\varphi}\cdot T\rangle\ll 2\pi$, where T is the time taken for image synthesis. However, in a day, ρ_e, ρ_p, and δ vary because of tides, the motion of the pole in the body of the Earth, and the precession-nutation movement of the Earth. These changes can be precalculated only with a restricted accuracy, which may prove insufficient in constructing images with high angular resolution. For example, for an interferometer with an equatorial baseline $\rho_e=3000$ km, $\rho_p=0$ with a resolution of 5×10^{-10} and $\lambda=5$ cm, we must have $\langle\Delta\dot{\varphi}\cdot T\rangle\leq 10°$. Then we require in the precalculation of $\Delta\varphi_{\text{geom}}$ that $\langle\rho_e\rangle/\rho_e\cdot T$, $\langle\dot{\delta}\rangle\cdot T\leq 10^{-8}\approx 0.002''$ ($\delta_2-\delta_1=2°$, $\delta_2=45°$). This is impossible within the framework of the existing theories.[85]

Therefore, in constructing images by the reference-object method, we require data of exact coordinate and geodynamic measurements (Secs. 4, b, 2 and 4, b, 3).[11)]

2) *"Closure phase" method.* If one simultaneously observes a source with a multielement, e.g., three-element radiointerferometer, then the sum of the phases of the signals of each of the two-element interferometers contained in the complex (the "closure phase") will equal the sum of the phases of the corresponding visibility functions: (the subscripts denote the stations)

$$\arg R_{12}+\arg R_{23}+\arg R_{31}=\varphi(\mathbf{w}_{12})+\varphi(\mathbf{w}_{23})+\varphi(\mathbf{w}_{31}). \quad (24)$$

It will not contain differential phase shifts of instrumental or atmospheric origin, nor the total geometric phase, since $\rho_{12}+\rho_{23}+\rho_{31}=0$.

The uncertainty in the image thus obtained reduces only to a shift in the reference origin, which is not essential to the form of the image.[12)] Actually, let $I_1(\sigma)$ and $I_2(\sigma)$ have values such that $|V_1|=|V_2|$, and

$$\varphi_1(\mathbf{w}_{12})+\varphi_1(\mathbf{w}_{23})+\varphi_1(\mathbf{w}_{31})=\varphi_2(\mathbf{w}_{12})+\varphi_2(\mathbf{w}_{23})+\varphi_2(\mathbf{w}_{31})+2\pi m.$$

Then $\Delta\varphi=\varphi_1-\varphi_2$ satisfies the condition: $\Delta\varphi(\mathbf{w}_{12})+\Delta\varphi(\mathbf{w}_{23})+\Delta\varphi(\mathbf{w}_{31})=2\pi m$, or $z(\mathbf{w}_{13})=z(\mathbf{w}_{12})\,z(\mathbf{w}_{23})$,

11) When the angular distance between the reference and studied sources is $\Psi\ll1$, then we have $\Delta\varphi_{\text{geom}}\ll1$, and the requirements on the quality of the coordinate information are substantially relaxed.

12) For the concrete algorithms, see Refs. 33, 69, and 72.

where $z(\mathbf{w}) = \exp[j\Delta\varphi(\mathbf{w})]$. This implies that $z(\mathbf{w}) = \exp(j\mathbf{A}\cdot\mathbf{w})$, where $\mathbf{A}$ is a certain vector such that $\varphi_1(\mathbf{w}) = \varphi_2(\mathbf{w}) + \mathbf{A}\cdot\mathbf{w}$ for all $\mathbf{w}$. Consequently we have $V_1(\mathbf{w}) = V_2(\mathbf{w})\exp(j\mathbf{A}\cdot\mathbf{w})$, and $I_1(\sigma) = {}^2F(V_1) = I_2(\sigma - \mathbf{A})$.

Evidently, in constructing the image of a radio source by the "closure phase" method we need not know its coordinates. However, in order to locate the obtained image, we require independent exact coordinate measurements.

3) *Multifrequency method.* According to (8), the argument of the interference signal can be represented in the form

$$\arg R = \varphi(u, v) + \mu f + \varphi^*_{\text{app}}. \tag{25}$$

Here μ contains all the terms whose phase shifts are proportional to the frequency of observation, and φ^*_{app} is the constant component of the instrumental phase shift, which involves, in particular, the initial desynchronization of the time scales.

If one observes a source at two frequencies f_1 and f_2 under the condition that the heterodynes at each of the stations are synchronized from a single frequency standard, then we have, to the accuracy of the constant component:

$$\arg R_1 - \xi \arg R_2 \equiv \Phi(u, v) = \varphi_1(u, v) - \xi\varphi_2(u, v). \tag{26}$$

Here $\xi = f_1/f_2$, and the subscripts denote the different frequencies. If we assume that the spatial image of the source if the same at the frequencies f_1 and f_2, we have $\varphi_2(u, v) = \varphi_1\left(\frac{1}{\xi}u, \frac{1}{\xi}v\right)$, and hence,

$$\Phi(u, v) = \varphi_1(u, v) - \xi\varphi_1\left(\frac{1}{\xi}u, \frac{1}{\xi}v\right). \tag{27}$$

If data on the function $\Phi(u, v)$ exist at many points of the uv plane, then we can reconstruct an approximate value of the phase of the visibility function:

$$\varphi_1(u, v) \approx \sum_{k=0}^{p} \xi^k \Phi\left(\frac{1}{\xi^k}u, \frac{1}{\xi^k}v\right). \tag{28}$$

Since the rms error of reconstruction of the phase is $\langle\varphi_1\rangle \propto (1/\sqrt{\xi - 1})\langle\sigma\rangle$, where $\langle\sigma\rangle$ is the fluctuational sensitivity of the interferometer in terms of flux, evidently the multifrequency method proves more effective as f_1/f_2 increases. However, in the general case the spatial radio brightness distribution can depend substantially on the frequency. This limits the region of applicability of the multifrequency method.

4) *Supersynthesis of two-dimensional images.* The quality of the image is determined by the degree of filling of the uv plane and by the signal-to-noise ratio Q in each of its discrete cells. Evidently only a multielement system operating in a network regime can fill the uv plane densely enough with a relatively small number N of telescopes, i.e., produce a diagram having a relatively small number of sidelobes. In an N-element system the total number of baselines is $N(N-1)/2$, part of which are not independent (the so-called redundancy of the system). Evidently the optimal system is the one with minimal redundancy for the given number of elements, since it brings about the best filling of the uv plane, and hence the greatest sensitivity to details of the image having a broad spectrum of angular scales. However, the redundancy of the system is *per se* not a negative property, since it allows one to increase Q in the corresponding cell in the uv plane. This is important in synthesizing images of sources having small fluxes.

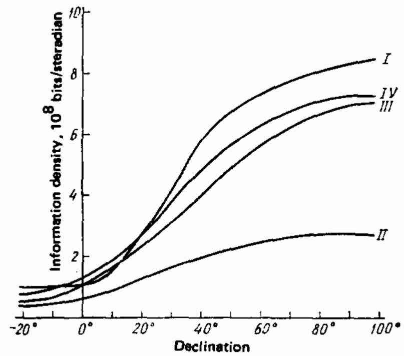

FIG. 18. Comparison of multielement systems in information content (from Table III).

The relative arrangement of the elements of the system determines its potentialities in constructing two-dimensional images of sources having different declinations. In particular, one-dimensional lattices oriented in an East-West direction (such as the 3-element 1-mile and 8-element 5-km interferometers at Cambridge and the 12-element 1-mile interferometer at Westerbork) allow one to synthesize images only of circumpolar sources with 12-hour tracking. Generally a two-dimensional lattice requires a larger number of antennas for a given level of sidelobes of the synthetic diagram than a one-dimensional lattice does. However, only the former can produce two-dimensional images of sources having arbitrary declinations. The choice of the relative arrangement of the elements constitutes a nontrivial problem, even for a one-dimensional lattice, since the different variants allow one to "emphasize" details of sources having different scales.[73] One can use the information content, which allows one to compare systems with different configurations, as a convenient characteristic of the filling of the uv plane[74]:

$$I = \frac{1}{2}\sum_{i,j} \log_2(1 + Q_{ij})\,\Delta u_i \Delta v_j. \tag{29}$$

Here Q_{ij} is the signal-to-noise ratio in the ij cell of the discrete uv plane having the dimensions $\Delta u_i \Delta v_j$.

Figure 18 shows as an example the variations of the information density per steradian for systems having different configurations (Table III) that can be formed within the territory of the USSR[13)] in observing a source of angular dimension 0.01″ at different declinations. Figure 19 shows the character of the filling of the spatial-frequency plane for system I. We see that one can create a system for dense filling of the uv plane with a relatively small number of elements.

---

13)Table III includes Warsaw, a station that allows extension of the network in longitude.

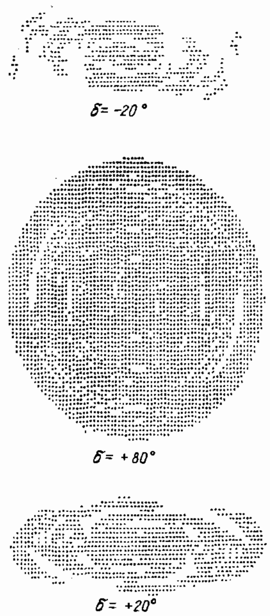

FIG. 19. Covering of the uv plane for system I (from Table III).

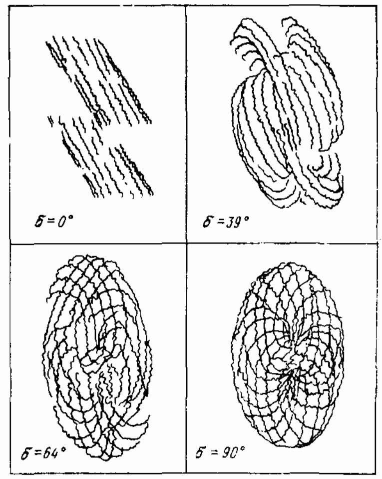

FIG. 20. Covering of the uv plane by the RAKSAS system ($H_s = 350$ km, $P = 24^h$).

In supersynthesis, which employs the diurnal rotation of the Earth, the projection of the baseline of the interferometer yields only one track in the uv plane in 12 hours. Therefore the percent of filling of the uv plane can be raised only by increasing the number of elements forming the system. A substantially different situation will exist if one includes in the system even one space-borne telescope—a system of the type of RAKSAS.[75] The relative motion of the Earth and of the space radiotelescope leads to a substantially larger set of projections of baselines than in the case of a system of rigidly fixed ground-based radiotelescopes. In line with this, the filling of the spatial-frequency plane of even a two-element system (ground-based + space-borne radiotelescopes) for a diurnal synthesis is no poorer than the filling of a multielement (up to 10 antennas) ground-based system (Fig. 20). It can be improved utilizing the precession of the orbit for prolonged intervals of synthesis. Because of this property a system including a space-borne element presents a qualitatively new idea in constructing aperture synthesis systems.

Evidently a system would be ideal for constructing images that has a structure that can adapt in resolution and redundancy to some particular problems or objects. However, such a potentiality can be partly realized only in interferometry with small baselines and with mobile elements. An example of such a lattice is the two-dimensional 27-element VLA system.[52] Therefore the optimal system seems to be successive synthesis of "international maps" of radio sources performed by combining in a computer all the two-dimensional images of the same radio source obtained with ever increasing resolution (Table IV).

TABLE III. Examples of variants of multielement systems.

Stations	Variants I	Variants II	Variants III	Variants IV	Stations	Variants I	Variants II	Variants III	Variants IV
Warsaw		+		+	Gor'kiĭ		+	+	+
Uzhgorod		+			Ashkhabad	+			+
Kishinev	+				Tashkent	+	+	+	
Leningrad		+	+		Alma-Ata	+			+
Murmansk		+	+	+	Novosibirsk				+
Evpatoriya	+				Tomsk			+	
Simeiz		+			Irkutsk	+		+	+
Moscow		+	+		Vladivostok	+		+	+
Zelenchukskaya	+	+	+	+	Yuzhno-Sakhalinsk	+			

b) Measurement of the coordinates of point sources and geodynamic parameters

The existing methods of measuring coordinates and geodynamic parameters can be divided into three groups: a) the absolute method,[76-79] b) the differential method,[67,79,80] and c) the method of arcs.[81-85] As we shall see below, these methods differ from one another in the degree of utilization of such *a priori* information as the geodynamic and geophysical model of the Earth, the model of the standards and of the atmosphere, and consequently, in their potential accuracy. Various observational programs and algorithms for processing the secondary information are used to realize them.

1) *Absolute method.* This method solves the coordinate and geodynamic problems by the simplest means. According to (6) and (7), we can write the fundamental equations of this method in the form

TABLE IV. A possible variant of sequential synthesis of "international maps of radio sources".

Country	System	Region in the uv plane in λ	Remarks
West Germany	Bonn radiotelescope	$0-2\cdot 10^3$	Operating since 1972
USSR	RATAN-600	$0-1.7\cdot 10^4$	Operating since 1974
USA	VLA	$10^4-7\cdot 10^5$	Operating since 1979
Europe	ESA system	$10^6-5\cdot 10^7$	Project
USA	National network	up to 10^8	Project
USSR	Poligam	up to 4×10^8	Project
USSR	Poligam + RAKSAS	up to 10^{13}	Project

$$\tau=(A+p)+\sqrt{B^2+C^2}\cos\left(\Omega t+\tan^{-1}\frac{C}{B}\right)+qt,\quad \varphi=\frac{2\pi}{\lambda}c\tau \tag{30}$$

and

$$f^{-1}F=-\Omega\sqrt{B^2+C^2}\sin\left(\Omega t+\tan^{-1}\frac{C}{B}\right)+q. \tag{31}$$

Here we have $A=(1/c)\ \rho_p\sin\delta, B=(1/c)\ \rho_e\cos\ \delta\cos\beta_0$, and $C=(1/c)\ \rho_e\cos\ \delta\sin\beta_0$. Also, β_0 is the value of the parameter $\beta=s-\alpha-\Lambda=\alpha_b-\alpha$ at the instant $t=0$, and p and q are corrections that take into account the initial shift of the local time scales and their relative rate difference. Four groups of parameters figure in Eqs. (30) and (31): a) parameters of the source: α, δ_b; b) parameters of the interferometer: ρ_e, ρ_p, and Λ, or $\rho^2=\rho_e{}^2+\rho_p{}^2$, Λ, and δ_b; c) instrumental parameters: p and q; and d) parameters of the Earth: Ω and α_b^0. Not all of them are independent. In particular, in interferometric observations one cannot separate α, Λ, and α_b^0—only β_0 is determined by them. Thus radiointerferometric measurements do not enable one to fix the null point of the system of right ascensions of the sources.

Evidently one can make for a fixed source only five independent readings of τ, which determine the amplitude, frequency, and initial phase of the sinusoidal component of τ, and also the magnitude of the displacement and the slope of its linear component, and four readings of F. In addition to Ω and q, the measurements of τ will give for each of the N sources the values of $A+p$, B^2+C^2, and C/B, i.e., three independent equations containing five independent parameters: ρ_e, ρ_p, p, β_0, and δ. In order for this system to be solvable, one must observe a minimal group of three sources ($3N>2N+3$).

In the absolute method, in order to create a solvable system, one must make two highly essential assumptions, which restrict its accuracy in principle. First, one must assume that the troposheric correction is known from indirect measurements of meteorological data. Since the regular component can be well precalculated,[86] the basic uncertainty is introduced by the random fluctuations of the eikonal. Second, one must model the deviation of the local time scales by some expansion, e.g.,:

$$\Delta\tau_{app}=p+qt. \tag{32}$$

Thus the actual accuracy of determining coordinates and other parameters is restricted by the accuracy of the adopted model and the choice of the program of observations.

The optimal program yielding the best resolution of the system depends primarily on the orientation of the instrument and the time that the sources remain in its overall visibility zone, i.e., ultimately on the duration T of the session. In order to attain the maximum accuracy in separating the variables, we must have $T\approx 12$–24 hours. Unfortunately this requirement is antagonistic to the model (32). Actually, with an instability of the standards of 10^{-13}–10^{-14}, the irregular deviation of the two scales in 12 hours will be of the order of 5×10^{-9}–5×10^{-10} s (150–15 cm). Yet taking into account a larger number of terms of the expansion of $\Delta\tau_{app}$ will entail an increased number of parameters to be determined, and consequently reduce the accuracy of determining them.[80] For the reasons cited above, the accuracy of the absolute method is limited to 0.1″–0.05″ for an instability of the standards of 5×10^{-13}–5×10^{-14}. When one employs standards with higher long-term stability, the main factor limiting the accuracy of the method is the fluctuation of the eikonal.

2) *Differential method.* The idea of this method is presented qualitatively in Sec. 3, b, 3. Here we shall briefly discuss the algorithm to be applied in coordinate measurements. If we generate the differential time lag τ_{12}, then according to (6) we shall have

$$\tau_{12}=A_{12}+B_{12}\cos(\Omega t+\gamma_{12}+\alpha_b^0). \tag{33}$$

Also, if the right ascensions of the sources are referred to the reference source, then we have

$$A_{12}=\frac{1}{c}\rho_p(\sin\delta_1-\sin\delta_2), \tag{34}$$

$$B_{12}=\frac{1}{c}\rho_e\sqrt{\cos^2\delta_1+\cos^2\delta_2-2\cos\delta_1\cos\delta_2\cos(\alpha_2-\alpha_1)},$$
$$\gamma_{12}=\tan^{-1}[\cos\delta_1\cdot\sin(\alpha_2-\alpha_1)(\cos\delta_1\cos(\alpha_2-\alpha_1)-\cos\delta_2)^{-1}]. \tag{35}$$

Accumulation of four independent readings of τ_{12} allows one to determine A_{12}, B_{12}, $\Phi_{12}=\alpha_b^0+\gamma_{12}$, and Ω. From this point, it is convenient to construct the algorithm of the method so as to eliminate the direct determination of α_b^0. If we observe three sources in pairs and find the corresponding differences Φ_{ik}, then the difference

$$\Phi_{12}-\Phi_{13}=\tan^{-1}\frac{\cos\delta_2\sin(\alpha_2-\alpha_1)}{\cos\delta_2\cos(\alpha_2-\alpha_1)-\cos\delta_1}-\tan^{-1}\frac{\cos\delta_3\sin(\alpha_3-\alpha_1)}{\cos\delta_3\cos(\alpha_3-\alpha_1)-\cos\delta_1} \tag{36}$$

will not depend on the orientation of the baseline vector in the equatorial plane. Finally, if we observe N sources forming $N-1$ independent pairs, then, in order to solve the system (33)–(36) for ρ_e, ρ_p; δ_i, and $\alpha_i-\alpha_1$, we must have $2(N-1)+(N-2)\geqslant 1+2N$. Consequently the minimum group of sources needed to realize the method is $N\geqslant 5$. These sources must be observed in pairs, and each pair must be observed at least at four instants of time, with the reference source taking part in each pair.

Whenever prior information exists on the sources, the problem of determining the parameters of the baseline of the interferometer is solved by pairwise observation of only three sources as a minimum at four instants of time, in line with the relationship

$$4\sin^2\frac{\Psi_{ij}}{2}=\frac{(A_i-A_j)^2}{(\rho_p/c)^2}+\frac{(B_i-B_j)^2+(C_i-C_j)^2}{(\rho_e/c)^2}. \tag{37}$$

Here Ψ_{ij} is the relative angular distance between the sources.

Formally the accuracy of the differential method is very high. With restrictions on the baseline that are not too strong, it can amount to a fraction of a millisecond of arc. However, the algorithm of the method is constructed in such a way that its realization generally requires a half-day or full-day accumulation of information on the differential values of τ_{ij}. Here one must assume that the parameters to be determined (ρ_e, ρ_p, Ω, and δ) are stationary within this time interval.[14] Of course this does not correspond to reality when one is speaking of accuracies of the order of a millisecond of arc and higher. In the reduction of the values of τ_{ij} to a single system, the accuracy of determining the unknowns will ultimately depend on the amount of detail in which we know the precession-nutation motion of the Earth, and the motion of the pole and of the points of the Earth's crust. However, a large fraction of the parameters characterizing these effects cannot be obtained from independent observations, while their precalculated values depend substantially on *a priori* physical models of the internal structure of the Earth, and primarily of its core. For example, the values determined by the various theories of the principal coefficients of nutation differ from one another in the range 0.02–0.04″.[85] Moreover, we must not ignore the possible short-term effects in the motion of the Earth's axis and of the baseline vector involving mantle-core relationships, and also of the Earth's surface and the ocean, tectonic activity, etc., which are impossible in principle to precalculate.

In this situation, just as in the absolute method, the pure coordinate problem in the differential method becomes inseparable in principle from the geophysical and geodynamic problems. A way out of this situation had already been proposed in optical astronomy[88]—one must reject the equatorial system of coordinates and go over to a system resting on the mutual angular distances between the sources (arcs). The arcs are invariants of the rotation, and do not depend on the translational-rotational motion of the Earth and the behavior of the baseline.

3) *Method of arcs.* In essence, the solution of the problem formulated above reduces to constructing a resolvable system that will allow one to determine the arcs, in a certain sense, independently of a knowledge of the orientation of the vectors ρ and $\mathbf{\Omega}$, i.e., ultimately by a purely geometric method. Then the problems involving the behavior of ρ and $\mathbf{\Omega}$, which have an especially geophysical and geodynamic content, will be solved as inverse problems to the purely geometric problem of determining the arcs.

Let us show on a simple example that this problem can be solved, though it requires considerably more effort than the coordinate measurements in the absolute and differential methods. Let us perform a series of simultaneous (we can easily take quasismultaneity into account for short intervals of time by using the rotation matrix) measurements of N sources and find the differences:

$$c\tau_{j0} = \boldsymbol{\rho}\,(\mathbf{k}_j - \mathbf{k}_0) \equiv \boldsymbol{\rho}\,\Delta\mathbf{k}_j, \quad j = 1, 2, \ldots, N-1. \tag{38}$$

If we use, e.g., the first three equations of the system (38), we can obtain an expression for the nonstationary vector ρ:

$$\frac{1}{c} V\boldsymbol{\rho} = \tau_{10}\,[\Delta\mathbf{k}_2 \times \Delta\mathbf{k}_3] + \tau_{20}\,[\Delta\mathbf{k}_3 \times \Delta\mathbf{k}_1] + \tau_{30}\,[\Delta\mathbf{k}_1 \times \Delta\mathbf{k}_2], \qquad V = \Delta\mathbf{k}_1\,[\Delta\mathbf{k}_2 \times \Delta\mathbf{k}_3]. \tag{39}$$

By using it, we can eliminate ρ from the remaining $N-4$ equations of (38). Consequently we obtain a system containing only quantities stationary and invariant with respect to three-dimensional rotations:

$$\tau_{j0} = V^{-1}\,\{\Delta\mathbf{k}_j \cdot \Delta\mathbf{k}_2 \times \Delta\mathbf{k}_3\;\; \tau_{10} + \Delta\mathbf{k}_j \cdot \Delta\mathbf{k}_3 \times \Delta\mathbf{k}_1\;\; \tau_{20} + \Delta\mathbf{k}_j \cdot \Delta\mathbf{k}_1 \times \Delta\mathbf{k}_2\;\; \tau_{30}\}; \quad j = 4, 5, \ldots, N-1. \tag{40}$$

Each of the equations of this system can be redetermined independently at three instants of time, thus determining the generalized parameters:

$$\Delta\mathbf{k}_j\,[\Delta\mathbf{k}_1\,\Delta\mathbf{k}_2]\,V^{-1}, \quad \Delta\mathbf{k}_j\,[\Delta\mathbf{k}_2\,\Delta\mathbf{k}_3]\,V^{-1}, \quad \Delta\mathbf{k}_j\,[\Delta\mathbf{k}_1\,\Delta\mathbf{k}_3]\,V^{-1}. \tag{41}$$

These parameters are related in an evident fashion to the arcs:

$$\Delta\mathbf{k}_i\,(\Delta\mathbf{k}_j\Delta\mathbf{k}_l) = \begin{vmatrix} \Delta\mathbf{k}_i^2 & \Delta\mathbf{k}_i\Delta\mathbf{k}_j & \Delta\mathbf{k}_i\Delta\mathbf{k}_l \\ \Delta\mathbf{k}_j\Delta\mathbf{k}_i & \Delta\mathbf{k}_j^2 & \Delta\mathbf{k}_j\Delta\mathbf{k}_l \\ \Delta\mathbf{k}_l\Delta\mathbf{k}_i & \Delta\mathbf{k}_l\Delta\mathbf{k}_j & \Delta\mathbf{k}_l^2 \end{vmatrix}^{1/2}, \tag{42}$$
$$\Delta\mathbf{k}_i\Delta\mathbf{k}_j = 1 + \cos\Psi_{ij} - \cos\Psi_{i0} - \cos\Psi_{j0}.$$

Consequently, in order for the system (40) to be solvable for the $2N-3$ independent arcs, the condition must be satisfied that $3(N-4) \geq 2N-3$. Thus, in order to determine coordinates by the geometric method while using only phase information, one must observe synchronously or quasisynchronously nine sources according to one of two programs:

a) nine sources having the unit vectors $\mathbf{k}_0$–$\mathbf{k}_8$ at three instants of time; b) all possible quintets of sources formed by adding to the four reference sources 0–3 one of the sources 4–8 at three instants of time. One can decrease the number of sources needed for solvability of the system by forming the differences F_{ij} in parallel with τ_{ij}. In this case the minimum group of sources is $N=5$, and one must observe it, at a minimum, at four instants of time.[83]

In the quasisimultaneous observations of 5–9 sources with modern full-rotation antennas, the length of the session will not exceed an hour. Within this interval one can guarantee the stationarity of ρ and $\mathbf{\Omega}$ with an accuracy of fractions of a millisecond of arc, while taking into account the nonsimultaneity of the observations within the framework of the model of a uniformly rotating Earth and the first-order theory of the tides. Evidently one can guarantee the constancy of p within this interval to an accuracy of fractions of a nanosecond by employing standards having an instability no worse than 10^{-13}.

It is very useful in solving coordinate problems to employ multielement interferometers, since this diminishes the necessary number of observations of the minimal group of sources. This is important in connection with the strongly restricted total zone of visibility involved with large baselines. In particular, when one uses a 4-element interferometer (three independent baselines), observations of the sources at only one instant of time suffice.[84,82]

As the example given above implies, the solution of a coordinate problem in the method of arcs proves to be a methodologically rather complicated problem. Yet the operation of such a system is attained by considerably simpler means. Actually, if we know the arcs be-

---

[14] This situation is also characteristic of the absolute method, which requires stationarity of ρ_e, ρ_p, β_0, δ, p, and q.

tween the reference sources 0–3, we can reconstruct by observations of them the instantaneous values (to the accuracy of the session duration $T \approx 30$ min) of the vectors ρ and $\mathbf{F} = \mathbf{\Omega} \times \mathbf{e}$. Hence we can determine the parameters of the interferometer and the vector $\mathbf{\Omega}$.

Thus, with a stagewise solution of the coordinate, geodynamic, and geophysical problems, it becomes possible not only to increase the potential accuracy in determining ρ and $\mathbf{\Omega}$, but also to study the high-frequency components of their spectra.

5. OPTIMAL STRUCTURE OF THE INTERFEROMETRIC NETWORK

One of the most brilliant illustrations of the close connection between the problems of constructing two-dimensional images and determining the positions of cosmic sources is the fact that the problems of both groups impose very similar requirements on the geometry and composition of the multielement radiointerferometric complex.

a) Reference sources

The reference-object method constitutes the central idea whose practical realization enables one to create a phase-stable interferometric system. It can be applied equally effectively both to problems involving construction of images and to those of determining the coordinates of sources (within the framework of the differential method and the method of arcs). Thus it is favorably distinguished from the "closure phase" method.

Evidently the successful realization of the reference-object method depends on the number of sources having a given flux per unit area of the celestial sphere that can be used to eliminate random phase shifts, primarily of tropospheric origin. At present VLBI observations have covered about 600 compact ($\leq 0.01''$) extragalactic radio sources. However, complete and systematic surveys at high resolution do not yet exist. Therefore, in order to estimate the density surfaces of compact sources, one must rely on indirect arguments, such as the variability of the sources, their spectral properties, and scintillation of their radio brightness due to inhomogeneities in the interplanetary plasma. Estimates resting on such arguments have been made[89] on the basis of a statistical analysis of the survey[90] at the wavelength $\lambda = 6$ cm. For sources with fluxes $F_{\min} \gtrsim 0.05$ Jy they showed that the surface density of such sources having details with angular dimensions smaller than $0.001''$ must be no less than 1500/steradian, so that the "flux-number of sources" relationship in the centimeter range of wavelengths has the form

$$F_{\min} = F_0 \left(\frac{n_0}{n}\right)^{2/3}. \tag{43}$$

Here we have $F_0 = 0.1$ Jy and $n_0 = 50$. This relationship is important in principle for estimates of the potentialities of the reference-object method, since for a given $F_{\min}$ it enables one to estimate the maximum angular distance $\Psi \approx \sqrt{1/n}$ between the reference source and the sources to be studied for which the fluctuational phase shift of the response due to tropospheric inhomogeneities proves to be negligibly small.

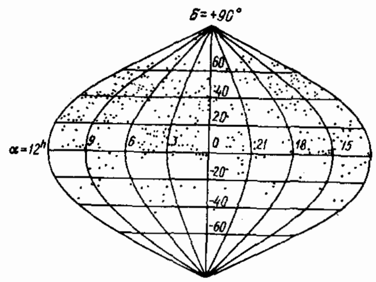

FIG. 21. Positions of candidates for extragalactic point sources.

Figure 21 shows the positions in the equatorial system of coordinates of the candidate point sources with fluxes $F \gtrsim 0.05$ Jy. In particular, they include sources having flat or complex spectra, and also variable sources.[91]

b) Optimal baselines of the interferometric network

While the need of long baselines $\rho > L_2$ arouses no doubts as applied to problems of constructing images of sources at high resolution, the opposite viewpoint is widespread with regard to coordinate problems. At first glance it seems that one can realize high coordinate resolution in determining positions with small baselines ($\rho \lesssim 100$ km) by employing the differential method. Actually the phase-closure problem is not so severe with small baselines as in VLBI (in any case, in the centimeter range). First, direct communication between the stations is possible with small baselines (waveguides, radio relay lines, fiber optics). Second, the tropospheric shift in the eikonal for these baselines is $\sqrt{D_t(\rho)} < 2.5$ cm. The measurement of the phase to 1° (to small fractions of λ/ρ) can be realized by differential measurements. Unfortunately, this attractive potentiality is not realizable in practice, since it requires extremely high flux sensitivity of the system, and consequently antennas of monstrous dimensions. Let us present the estimates confirming this viewpoint. To do this, we shall examine the ideal case in which the sources are observed with a two-element interferometer at the same angles at both points, while the time of data accumulation is $T > t_1$. Then, according to (9), (10), and (19), the variance in the determination of direction involving the tropospheric noise and the instrumentation is given by the following expression for phase observations on sources having the same flux:

$$\langle \theta^2 \rangle \approx \frac{2\lambda^2}{4\pi^2 \rho^2 Q^2} + \frac{C_T^2 \Psi^2}{\rho^2}. \tag{44}$$

Here we have $Q = (\pi\sqrt{2\Delta f T}/32kT_{\text{noise}})\, d^2 F_{\min}$ and $C_T = C_L/(vT)^{2/3} \cos z$. Evidently for large Ψ the error $\langle\theta\rangle$ is governed (for a given flux sensitivity) by tropospheric effects, while for small Ψ it is governed by the additive noise of the apparatus. Hence one can find a Ψ value at which the goniometric error is minimal.

By using (43), we can find the optimal angular distance between sources having fluxes $F_{\min}$:

$$\Psi \approx \sqrt{\frac{1}{n}} = \frac{1}{\sqrt{n_0}} \left(\frac{F_{\min}}{F_0}\right)^{3/4}. \tag{45}$$

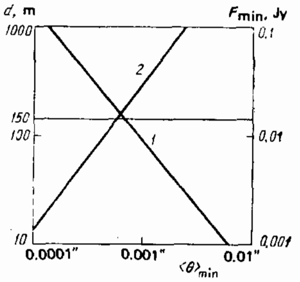

FIG. 22. Dependence of the limiting angular resolution on the antenna diameter for an interferometer of 40-km baseline. 1—diameter of antennas, 2—flux of the source used as the reference.

Then, taking (44) and (45) into account, we have the following expression for the minimal error of angular measurement:

$$\langle\theta\rangle_{min} \approx 0.3\,\frac{\lambda}{\rho Q_{opt}}, \quad Q_{opt} \approx 0.1\beta^{2/7} d^{6/7}. \tag{46}$$

Here we have

$$\beta = \frac{\lambda^2}{C_T^2}\, n_0 F_0^{3/2} \left(\frac{\pi\sqrt{2\Delta f T}}{32kT_{noise}}\right)^{3/2}.$$

Let us assume the following parameters of the T_{noise} system for numerical estimates: $\rho = 40$ km, $\Delta f = 50$ MHz, $T_{noise} = 50$ K, $T = 1$ hr, $\lambda = 5$ cm, and $z = 60^\circ$. Then we have

$$\langle\theta\rangle_{min} \approx 2.5\cdot 10^{-7} d^{-6/7}. \tag{47}$$

Thus, even in the optimal case, a coordinate resolution of the order of a millisecond of arc can be attained on a small baseline only when the diameters of the antennas of the interferometer are close to the limiting values $d \approx 100$ m. This is because one must observe sources with very small fluxes $F_{min} \lesssim 0.01$ Jy ($\Psi \lesssim 2^\circ$) for filtration of tropospheric inhomogeneities (Fig. 22). Therefore, baselines with $\rho > L_2$ are required for effective suppression of tropospheric effects. As for the upper bound of the baseline, we note first that it is not expedient to locate radiotelescopes at points extremely separated in longitude, since then prolonged tracking becomes impossible, even on objects with moderate declinations. From the standpoint of the problems of the first group, this means that a dense filling of the *uv* plane is impossible, i.e., the obtaining of a qualitative image in a day-long synthesis. From the standpoint of the problems of the second group, this sharply impairs the solvability of the corresponding systems of conditional equations. Moreover, the small common visibility zone of the system (small data accumulation time) diminishes its flux sensitivity. Analysis shows that the optimal arrangement of the elements of the network, which simultaneously looks after the problems of both groups, is attained when they are arranged at distances of $\sim R_\oplus$, rather than $2R_\oplus$. Thus the maximal separation of the elements in longitude should not exceed 80°–100°.

c) Number and dimensions of the elements of the interferometric network

The "polygamous ideology" requires one to select a certain number of elements so as to create an overall area of the system that will allow the sensitivity needed for effective application of the reference-object method. The central problem that one must solve in choosing the optimal structure of an N-element network is to determine the minimal number and dimensions of the antennas forming the phase-stable system. Let us examine this problem by starting with the requirement that a system with $T_{noise} = 50$ K and $\Delta f = 50$ MHz should allow determination of the position of sources with $\langle\theta\rangle = 0.0001''$ at the wavelength $\lambda = 5$ cm. First we shall determine the minimal total area of the system that can yield this resolution by applying the reference-object method.

By employing arguments analogous to those in Sec. 5b, we find that the minimal error of a single measurement of a position from the differential phase is

$$\rho\langle\theta\rangle_{min} \approx \frac{2}{Q_{opt}}, \quad Q_{opt} \approx \frac{(d^2\sqrt{N(N-1)})^{3/7} T^{3/14}}{5\alpha^{4/7}}. \tag{48}$$

Here α is the tropospheric shift in the eikonal, whose magnitude depends on the procedure of observing the reference sources. In line with the remarks in Sec. 5, b, we shall adopt as the characteristic dimension of the baseline $\rho \approx 3000$ km. Then, for $\langle\theta\rangle = 0.0001$, we have $Q_{opt} = 43$, and

$$d^2\sqrt{N(N-1)} \approx \frac{3\cdot 10^4 \alpha^{4/3}}{\sqrt{T}}. \tag{49}$$

Since the typical regime is one with large baselines in which the sources are observed at different zenith angles, then, according to (20), for $z \lesssim 60^\circ$, we can assume that

$$\alpha \leqslant \begin{cases} 22\text{ cm, if one does not measure the eikonal,} \\ 5\text{ cm, if one measures the eikonal.} \end{cases} \tag{50}$$

The time T of recording during which one must determine the differential phase is limited by two factors. First, one must guarantee within this interval the stationarity of all the geodynamic and instrumental parameters for observing the minimal group of sources. Second, the time T must be smaller than the characteristic period of the fluctuations of the eikonal. Both these requirements yield a similar estimate of $T = 600$ s. Then the "effective area" of the system that will allow the limiting angular resolution $\langle\theta\rangle = 0.0001''$ is

$$d^2\sqrt{N(N-1)} \approx \begin{cases} 7.5\cdot 10^4\,\text{m}^2\text{, if one does not measure the eikonal,} \\ 7.8\cdot 10^3\,\text{m}^2\text{, if one measures the eikonal.} \end{cases} \tag{51}$$

Hence we see the considerable role played by radiometric measurements of the electric thickness of the troposphere.

Evidently there is a multitude of variants for forming such a synthetic area (Fig. 23). The limiting variants among them are the "Tower of Babel" (large d, small N), and the "grand leap" (large N, small d), whose exact boundaries we shall try to establish below.

In order to choose the optimal combination of d and N, we must draw a picture, however qualitative, of the cost of each of them. If we treat the situation in most general outline, then the cost of the system consists of the cost of the antennas and that of the instrumentation,[52] which depend in different ways on d and N. Since

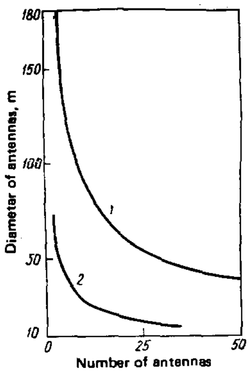

FIG. 23. "Diameter-number of antennas" relationship for a system having a limiting angular resolution of 0.0001. 1—The eikonal is not measured; 2—the eikonal is measured.

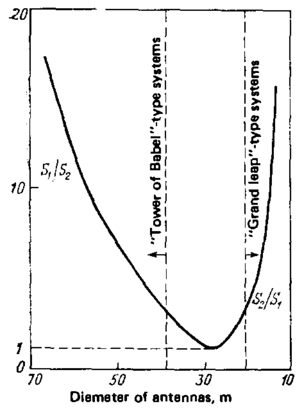

FIG. 25. Relationship between the expenses S_1 for the antennas and S for the instrumentation for different systems.

one generally assumes that the cost of the antennas is proportional to $d^{2.8}$,[92] then for a given effective area d^2N of the system the cost of its antenna component $S_A \propto Nd^{2.8} \propto N^{-0.4}$ declines with increasing N. On the other hand, the cost of the instrumentation component of the system increases with increasing N, so that an optimum in cost must exist between the "grand leap" and "Tower of Babel" variants.

Let us examine this situation in more detail by representing the cost S of the system in the following form (S is in arbitrary monetary units, and d in meters):

$$S = N\cdot 45\cdot\left(\frac{d}{70}\right)^{2.8} + N\,(1+0.1+0.5+0.05) + \frac{N\,(N-1)}{2}\,0.05 + N\frac{d}{70}. \tag{51$'$}$$

Here the first term represents the cost of the antennas, including the amortization expenses for 10 years, the second represents the cost of the instrumentation (in the following sequence: receivers, delay lines, stations for communicating with an artificial satellite, stations for measuring the eikonal), the third represents the cost of the correlators, and the fourth represents the operating expenses for 10 years.[15)]

Taking (50) into account for the case in which one performs measurements of the eikonal, we can easily see that a system of minimal cost can be built from 9–12 antennas with diameters $d = 30$–25 m (Fig. 24). It is interesting to note that antennas 25 m in diameter were chosen as the modular elements in the construction of the VLA system and in projecting the American and Canadian variants of the interferometric network.[6,9] We can easily see that the optimum in cost is reached when the expenses for the antennas are comparable with the expenses for the instrumentation (Fig. 25).

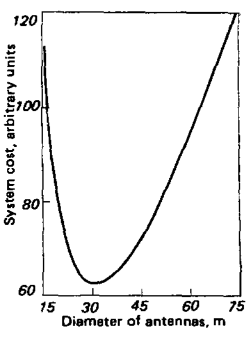

FIG. 24. Relationship of the cost of the system to the diameter of the antennas.

As we see from Fig. 26, systems made from antennas of relatively small dimensions are optimal also in cost per unit of information, which we can take to be the number of sources detectable per steradian. Table V gives the important parameters characterizing the optimal system, while Fig. 27 gives the statistical relationship [see (44)] of its angular resolution to the relative angular distances between the sources being observed.

We note that the idea of creating large interferometric systems out of relatively small elements is grasped psychologically with some difficulty. This reaction involves almost a half century of experience in radioastronomical observations in a radiometric regime that has fixed a tendency to constructing antennas of ever larger dimensions (an example of the extreme situation within the framework of this tendency is the uncompleted 180-m paraboloid in the USA[93]). However, as synthetic-aperture systems have appeared and operated successfully, the fact has become ever more evident that it suffices to see the sources in a network regime, and it is not at all obligatory to see them with the single antennas.

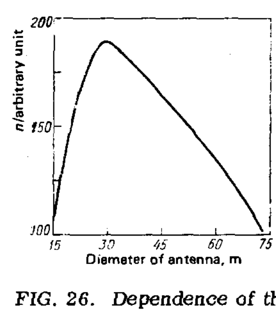

FIG. 26. *Dependence of the cost of information on the diameter* of the antennas.

15)The relative contributions of the components in (51′) are taken from the experience of designing a radiointerferometric network.

TABLE V. Fundamental parameters of the optimal system.

Diameter of antennas		30 m
Number of antennas		9
Cost ratio of antennas to instrumentation		1.3
Minimum detectable flux of a source	$(Q=5,\ T=600\ \text{s})$	2.6 mJy
Number of visible sources per steradian		10^4
Angular distance between sources	$(Q=5)$	0.52°
Number of sources per steradian whose positions can be determined with an accuracy of 0.0001″		480

In closing we note that the creation of large interferometric systems made of small elements is also optimal in the organizational sense, since each element of the system can play no substantial radioastronomical role when operating in an autonomous regime, and acquires significance only in operating in a network regime. The objective need of "cooperation over the collecting surface" can prove to be a highly essential factor for successful operation of the system, if we consider that its elements are separated by thousands of kilometers and are operated by independent scientific collectives that enter into contact only via a satellite channel.

d) Geometry of the interferometric network

In Sec. 5, b we discussed the longitude separation of the elements, while here we shall briefly discuss the problem of their latitude separation (two-dimensionality of the network). If we are discussing problems of constructing images, as we have noted, only a two-dimensional network can synthesize qualitative images of sources having moderate declinations. Yet if we are discussing problems of measuring coordinates, we must have a nonzero polar projection of the baseline, primarily based on the need to measure effects involving the motion of the pole.

The various methods of determining coordinates experience with differing sharpness the need for a baseline that has a polar projection. We shall illustrate this situation with the example of the method of arcs, for which separation in latitude is necessary in the highest degree (with an appreciable longitude separation). In the method of arcs the rms error $\langle \mathbf{k}_j \rangle$ in measuring coordinates with a two-element interferometer is[84]:

$$\langle \mathbf{k}_j \rangle = \sqrt{1+\Delta \mathbf{k}_j^2 K_s^2}\, K_b \langle \sigma \rangle. \tag{52}$$

Here $\langle \sigma \rangle$ is the fluctuational error in measuring the phase, K_s is a coefficient determined by the relative arrangement of the reference sources with respect to $\mathbf{k}_0$

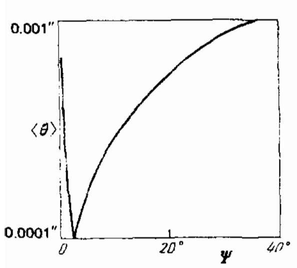

FIG. 27. Dependence of the resolving power of the optimal system on the angular distance Ψ between the sources.

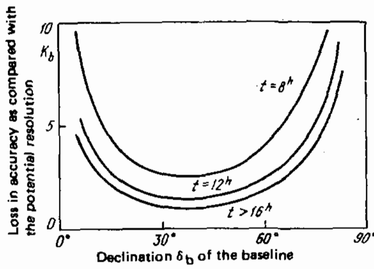

FIG. 28. Dependence of the accuracy of determining relative coordinates of sources on the declination δ_b of the baseline of the interferometer.

$-\mathbf{k}_3$, and K_b is a coefficient determined by the geometry of the radiointerferometer and the time t that the sources stay in the overall zone of visibility. If one employs only phase information, one has:

$$K_b^2 = \frac{2\sin^2\delta_b\,[3-2\cos(\pi t/T)-\cos(2\pi t/T)]+\cos^2\delta_b\,[2\sin^2(\pi t/T)+\sin^2(2\pi t/T)]}{3\sin^2\delta_b\cos^2\delta_b\,[2\sin(\pi t/T)-\sin(2\pi t/T)]^2}. \tag{53}$$

Here T is the length of the day. We see from (53) that measurements performed on a "polar" ($\delta_b = 90°$) or an "equatorial" ($\delta_b = 0°$) baseline do not allow one to determine the relative coordinates of sources.

In the special case in which $t \geq 16$ h (in particular with a source that does not set), we have

$$K_b^2 = \frac{4}{9\cos^2\delta_b} + \frac{1}{9\sin^2\delta_b}.$$

Then the optimal orientation of the baseline for which $K_b = 1$ corresponds to $\delta_b = 35°$. When $20° \lesssim \delta_b \lesssim 60°$, we have $1 \leq K_b \lesssim 1.4$ (Fig. 28). If $t < 16$ h, then the optimal declination of the baseline is determined by the condition

$$(\delta_b)_{\text{opt}} = \tan^{-1}\sqrt[4]{\frac{A(t)}{4A(t/2)}},\ \text{where}\ A(t) = \sin^2\frac{2\pi t}{T} + 2\sin^2\frac{\pi t}{T}.$$

Then, when $30° \lesssim \delta_b \lesssim 60°$ and $8\ \text{h} \lesssim t \lesssim 16$ h, we have $1.4 \lesssim K_b \lesssim 3.8$ (Fig. 28). Thus only a two-dimensional interferometric system possesses the necessary flexibility for solving various problems by different methods.

CONCLUSION

In the past decade, radiointerferometry with large baselines has made a number of advances whose significance in modern observational astrophysics and positional astronomy is difficult to overrate. In closing we wish to focus attention on the several fundamental ideas that constitute the common ground linking the national projects[6-9] (the fundamental characteristics of the national networks are given in Table VI).

First there is the idea of converting independent interferometry into "link-interferometry", which involves the vigorous development of the technology of digital intercontinental communication. For users, this conversion will imply the possibility of operating the system in the real time scale ("full day in real time") and the sharp expansion of the field of applicability of very-long-baseline interferometry for purposes of observational astronomy.

TABLE VI. Relative characteristics of the projected national radiointerferometric phase-stable networks.

Name of project / Basic characteristics:	VLBA (USA)	ESA (Europe)	Poligam (USSR)	CASCA (Canada)
Number N and diameter d of antennas	$N=10$, $d=25$ м	$N=10$, $d=15-100$ м	$N_1=3$, $d_1=70$ м $N_2=7$, $d_2=25$ м	$N=8$, $d=25$ м
Working wavelengths, λ (cm)	$\lambda=1.3$; 2; 6; 18; 21	Available on existing antenna	$\lambda=1.3$; 2.8; 8; 21	$\lambda=1.35$; 2; 6; 18; 21
Geometry of the network: longitude separation latitude separation	155 – 3°W 38 – 30°	3W – 34°E 40–60°	33 – 133°E 40–60°	54 – 125°W 49°
Angular resolution, seconds of arc	0.0005 ($\lambda=1.3$ cm)	0.001 ($\lambda=1.3$ cm)	0.0004 ($\lambda=1.35$ cm)	0.0004 ($\lambda=1.35$ cm)
Flux sensitivity in mJy for a receiving band Δf and recording time T	16 — 4 MHz — 20 m 4 — 56 MHz — 20 m	1 56 MHz 10 h	0.3 — 2 MHz — 12 h 0.04 — 100 MHz — 12 h	0.65 14 MHz 1 h
Noise temperature of the system, K	50	50	50	50
Clock synchronization principles	LORAN, OMEGA	Via satellite	LORAN, television, via satellite	LORAN
Principles of stabilization of heterodyne systems	1. Hydrogen standards 2. Superconducting resonator	1. Hydrogen standards 2. Via satellite	1. Hydrogen standards 2. Via satellite	1. Superconducting resonator 2. Via satellite
Signal-transmission system	Magnetic recording system MKIII, 28 channels, each 4 megabits/s	Via satellite-rate of transmission of one channel is 56 megabits/s	1. MKII-4 megabits/s 2. Via satellite	Magnetic recording on cassette videotapes. Recording band 3.5 MHz. 4–6 videotape recorders per station.

Second, there is the idea of building a "counteratmospheric" instrument by applying various methods for eliminating the phase instability of atmospheric origin and primarily—the reference-object method. Consequently it becomes possible to construct "true" radio images of celestial objects and to determine the coordinates of objects with an accuracy of small fractions of an interference lobe. Thus a radiointerferometric network with long baselines becomes equivalent to ordinary phase-stable synthetic-aperture systems.

Finally, there is the idea of combining radiotelescopes into a unitary network[94] capable of unbounded accretion in synthetic area, recording band, and frequency range.

Evidently such a global radiotelescope opens up a new era in the history of observational radioastronomy, enabling one to obtain unique observational information having general scientific significance. With the putting into operation of such a system, the exponential growth of radioastronomy that began in the fifties will apparently continue to the end of this century.

The authors thank their coauthors in the "Poligam" project,[8] many of the ideas of which have been employed in this article, and also N. L. Kaĭdanskiĭ for valuable comments.

[1]N. S. Kardashev, L. I. Matveenko, and G. B. Sholomitskiĭ, Izv. Vyssh. Uchebn. Zaved. Radiofiz. 8, 651 (1965).
[2]N. L. Kaidanovskiĭ, Radiotekh. Elektron. **10**, 1741 (1966).
[3]V. M. Chikhachev, *ibid.* **11**, 2072 (1966).
[4]N. W. Broten, R. W. Clarke, T. H. Legg, J. L. Locke, C. W. McLeish, R. S. Richards, J. L. Yen, R. M. Chisholm, and J. A. Galt, Nature **216**, 44 (1967).
[5]B. G. Clark, K. I. Kellermann, C. C. Bare, M. H. Cohen, and D. L. Jauncey, Astrophys. J. **153**, 705 (1969).
[6]K. Kellermann, An Intercontinental Very-long-base Array: VLBI Network Studies, III, NRAO, 1977.
[7]R. Schilizzi, J. O'Sullivan, K. Kellermann, W. Zing, J. Campbell, and G. Colombo, Very-long-baseline Radiointerferometry Using a Geostationary Satellite, ESA, Paris, 1978.
[8]V. A. Alekseev, S. Ya. Braude, V. A. Brumberg, Yu. D. Bulanzhe, É. D. Gatélyuk, G. B. Gel'freĭkh, V. S. Gubanov, A. F. Dravskikh, N. A. Esepkina, N. S. Kardashev, D. V. Korol'kov, B. A. Kotov, Yu. A. Kotov, G. A. Krasinskiĭ, A. B. Manukin, L. I. Matveenko, A. V. Men', V. N. Nikonov, N. N. Pariĭskiĭ, Yu. N. Pariĭskiĭ, S. V. Pogrebenko, E. I. Popov, V. A. Razin, A. E. Razin, A. E. Salomonovich, V. I. Slysh, S. G. Smolentsev, R. L. Sorochenko, K. S. Stankevich, A. A. Stotskiĭ, V. S. Troitskiĭ, N. D. Umarbaeva, A. M. Finkel'shteĭn, P. A. Fridman, V. K. Khersonskiĭ, G. S. Tsarevskiĭ, V. A. Tseĭtlin, V. N. Tsymbal, and Ya. S. Yatskiv, Proekt "Poligam" (The "Poligam" Project), Report of the Special Astrophysical Observatory of the Academy of Sciences of the USSR, No. 27-30 (1980).
[9]N. Broten, A. Bridle, J. Galt, P. Gregory, T. Legg, P. Kronberg, W. Shuter, and C. Costain, Preprint of the CASCA Committee on Radio Astronomy, 1979.
[10]R. D. Blandford and M. J. Rees, Mon. Not. RAS **169**, 395 (1974).
[11]G. Benford, *ibid.* **183**, 29 (1978).
[12]W. A. Christiansen, A. G. Pacholczyk, and J. S. Scott, Nature **266**, 593 (1977).
[13]W. C. Saslaw, M. J. Valtonen, and S. J. Aarseth, Astrophys. J. **190**, 253 (1974).
[14]K. I. Kellermann, D. B. Shaffer, G. H. Purcell, I. I. K. Pauliny-Toth, E. Preuss, A. Witzel, D. Graham, R. T. Schilizzi, M. H. Cohen, A. T. Moffet, J. D. Romney, and A. E. Niell, Astrophys. J. **211**, 658 (1977).
[15]K. I. Kellermann, D. B. Shaffer, I. I. K. Pauliny-Toth, E. Preuss, and A. Witzel, *ibid.* **210**, L121 (1976).
[16]V. I. Slish, Nature **199**, 682 (1963).
[17]J. Gubbay, A. J. Legg, D. S. Robertson, A. T. Moffet, R. D. Ekers, and B. Seidel, Nature **224**, 1094 (1969).
[18]C. A. Knight, D. S. Robertson, A. E. E. Rogers, I. I. Shapiro, A. R. Whitney, T. A. Clark, R. M. Goldstein, G. A. Marandino, and N. R. Vandenberg, Science **173**, 52 (1971).
[19]A. R. Whitney, I. I. Shapiro, A. E. E. Rogers, D. S. Robertson, C. A. Knight, T. A. Clark, R. M. Goldstein, G. E. Marandino, and N. R. Vandenberg, Science **173**, 225 (1971).
[20]K. I. Kellermann, D. L. Jauncey, M. H. Cohen, B. B. Shaffer,

B. G. Clark, J. Broderick, B. Rönnäng, O. E. H. Rydbeck, L. Matveyenko, I. Moiseyev, V. V. Vitkevich, B. F. C. Cooper, and R. Batchelor, Astrophys. J. **169**, 1 (1971).
[21]M. H. Cohen, W. Cannon, G. H. Purcell, D. B. Shaffer, J. J. Broderick, K. I. Kellermann, and D. L. Jauncey, *ibid.* **170**, 207 (1971).
[22]K. I. Kellermann, B. G. Clark, D. L. Jauncey, J. J. Broderick, D. B. Shaffer, M. H. Cohen, and A. E. Niell, *ibid.* **183**, L51 (1973).
[23]I. I. Shapiro, H. F. Hinteregger, C. A. Knight, J. J. Punsky, D. S. Robertson, A. E. E. Rogers, A. R. Whitney, T. A. Clark, G. E. Marandino, R. M. Goldstein, and D. J. Spitzmesser, *ibid.* **183**, L47 (1973).
[24]R. T. Schilizzi, M. H. Cohen, J. D. Romney, D. B. Shaffer, K. I. Kellermann, G. W. Swenson, Jr., J. L. Yen, and R. Rinehart, *ibid.* **201**, 263 (1975).
[25]A. E. Niell, K. I. Kellermann, B. G. Clark, and D. B. Shaffer, *ibid.* **197**, L109 (1975).
[26]M. H. Cohen, A. T. Moffet, J. D. Romney, R. T. Schilizzi, G. A. Seielstad, K. I. Kellermann, G. H. Purcell, D. B. Shaffer, I. I. K. Pauliny-Toth, E. Preuss, A. Witzel, and R. Rinehart, *ibid.* **206**, L1 (1976).
[27]K. Kellermann and D. Shaffer, in: Evolution of Galaxies and Its Application to Cosmology, IAU Sympos. No. 37, Paris, 1977, p. 347.
[28]M. J. Rees and M. Simon, Nature **227**, 1303 (1970).
[29]W. A. Dent, Astrophys. J. **175**, L55 (1972).
[30]R. Epstein and M. Geller, Nature **265**, 219 (1977).
[31]R. H. Sanders, Nature **248**, 390 (1974).
[32]L. É. Gurevich, A. F. Dravskikh, and A. M. Finkel'shteǐn, Astrofiz. Issled. **12**, 64 (1980).
[33]A. E. Rogers, H. F. Hinteregger, A. R. Whitney, C. C. Counselman, I. I. Shapiro, J. J. Wittels, W. K. Klemperer, W. W. Warnock, T. A. Clark, L. K. Hutton, G. E. Marandino, B. O. Ronnang, O. E. H. Rydbeck, and A. E. Niell, Astrophys. J. **193**, 293 (1974).
[34]J. J. Wittels, C. A. Knight, I. I. Shapiro, H. F. Hinteregger, A. E. E. Rogers, A. R. Whitney, T. A. Clark, L. K. Hutton, G. E. Marandino, A. E. Niell, B. O. Rönnäng, O. E. H. Rydbeck, W. K. Klemperer, and W. W. Warnock, *ibid.* **196**, 13 (1975).
[35]J. J. Wittels, W. D. Cotton, C. C. Counselman III, I. I. Shapiro, H. F. Hinteregger, C. A. Knight, A. E. E. Rogers, A. R. Whitney, T. A. Clark, L. K. Hutton, B. O. Rönnäng, O. E. H. Rydbeck, and A. E. Niell, *ibid.* **206**, L75 (1976).
[36]J. M. Moran, in: Frontiers of Astrophysics, Pergamon Press, New York, 1977, p. 385.
[37]T. A. Clark, L. K. Hutton, C. Ma, I. I. Shapiro, J. J. Wittels, D. S. Robertson, H. F. Hinteregger, C. A. Knight, A. E. E. Rogers, A. R. Whitney, A. E. Niell, G. M. Resch, and W. J. Webster, Jr., Astrophys. J. **206**, L107 (1976).
[38]D. Shaffer and R. Schilizzi, *ibid.* **80**, 753 (1975).
[39]B. Geldzahler, K. Kellermann, and D. Shaffer, *ibid.* **84**, 186 (1979).
[40]R. Vessot, in: Methods of Experimental Physics, Academic Press, New York, 1976, Vol. 12, Part C, Sec. 5.4.
[41]S. Refsdal, Mon. Not. RAS **128**, 307 (1964); Astron. **73**, 32 (1968).
[42]D. Walsh, R. F. Carswell, and R. J. Weymann, Nature **279**, 381 (1979).
[43]R. J. Weymann, F. H. Chaffee, Jr., M. Davis, N. P. Carleton, D. Walsh, and R. F. Carswell, Astrophys. J. **233**, L43 (1979).
[44]P. Young, J. Gunn, J. Kristian, J. Oke, and J. Westphal, Orange Preprint, CTI No. 587, Feb. 1980.
[45]K. S. Bhamra, A. M. Finkelstein, V. Ja. Kreinovich, and L. E. Gurevich, Astrophys. Space Sci. **57**, 371 (1978).
[46]B. Kolaczek and G. Weiffenbach, IAU Colloq. No. 26, Warsaw, 1975, p. 21.
[47]E. B. Fomalont and R. A. Sramek, Astrophys. J. **199**, 749 (1975).
[48]V. A. Brumberg and A. M. Finkel'shteǐn, Zh. Eksp. Teor. Fiz. **76**, 1474 (1979) [Sov. Phys. JETP **49**, 749 (1979)].
[49]N. S. Kardashev, Yu. N. Pariǐskii, and N. D. Umarbaeva, Astrofiz. Issled. **2**, 16 (1972).
[50]P. Connes, Opt. Tel. of the Future Conference Proc., ESO; CERN, 1977, p. 351.
[51]C. C. Counselman III, H. F. Hinteregger, and I. I. Shapiro, Science **178**, 607 (1972).
[52]VLA Concept, Vol. 1, NRAO, 1967.
[53]N. Broten, T. Legg, J. Locke, C. McLeish, R. Richards, R. Chisholm, H. Gush, J. Yen, and J. Galt, Science **156**, 1592 (1976).
[54]L. Gatterer, Trans. IEEE **IM-17**, 372 (1976).
[55]R. L. Iston, TIIÉR **64**, No. 10, 34 (1976).
[56]V. I. Tatarskiǐ, Rasprostranenie radiovoln v turbulentnoǐ atmosfere (Propagation of Radio Waves in a Turbulent Atmosphere), Nauka, M., 1967.
[57]A. A. Stotskiǐ, Radiotekh. Elektron. **18**, 1579 (1973).
[58]A. A. Stotskiǐ, Izv. Vyssh. Uchebn. Zaved. Radiofiz. **16**, 806 (1973).
[59]A. F. Dravskikh and A. M. Finkelstein, Astrophys. Space Sci. **60**, 251 (1979).
[60]A. F. Dravskikh, A. A. Stotskiǐ, A. M. Finkel'shteǐn, and P. A. Fridman, Astrofiz. Issled. **10**, 108 (1978).
[61]A. F. Dravskikh, A. A. Stotskiǐ, A. M. Finkel'shteǐn, and P. A. Fridman, Radiotekh. Elektron. **22**, 2305 (1977).
[62]Yu. N. Pariǐskiǐ and A. A. Stotskiǐ, Izv. GAO AN SSSR No. 188, 195 (1972).
[63]A. F. Dravskikh and A. M. Finkel'shteǐn, Astron. Zh. **56**, 1100 (1979) [Sov. Astron. **23**, 620 (1979)].
[64]J. Moran and H. Penfield, NASA Final Report NAS-5-20975, 1976; F. Winn, S. Wu, G. Resh, C. Chao, and O. von Roos, JPL Deep Space Network Progress Report No. 42–32, 1976; V. A. Alekseev, K. P. Gaǐkovich, and A. P. Naumov, in: Vliyanie atmosfery na astronomicheskie nablyudeniya (Effect of the Atmosphere on Astronomical Observations), Irkutsk, 1980, p. 19.
[65]N. Mathur, M. Grossi, and M. Pearlman, Radio Sci. **5**, 1253 (1970).
[66]N. A. Lotova, Usp. Fiz. Nauk **115**, 603 (1975) [Sov. Phys. Usp. **18**, 292 (1975)].
[67]V. A. Alekseev, Abstract of Candidate's Dissertation, NIRFI, Gor'kiǐ, 1970.
[68]R. C. Jennison, Mon. Not. RAS **118**, 276 (1958).
[69]D. N. Fort and H. K. C. Yee, Astron. Astrophys. **50**, 19 (1976).
[70]S. V. Pogrebenko, Preprint of the IKI AN SSSR No. 513, Moscow, 1979.
[71]S. von Hoerner, Astron. J. **72**, 35 (1967).
[72]O. M. Kosheleva, V. Ya. Kreǐnovich, and A. M. Finkel'shteǐn, in: Abstracts of Papers, 11th All-Union Radioastronomical Conference, Izd-vo AN Arm. SSR, Erevan, 1978, p. 220.
[73]A. Moffet, IEEE Trans. **NAP-16**, 172 (1968).
[74]D. V. Korol'kov and P. A. Fridman, Astrofiz. Issled. No. 2, 148 (1970).
[75]N. S. Kardashev, S. V. Pogrebenko, and G. S. Tsarevskiǐ, Preprint of the IKI AN SSSR No. 449, Moscow, 1978.
[76]P. Brosche, C. M. Wade, and R. M. Hjellming, Astrophys. J. **183**, 805 (1973).
[77]C. M. Wade, *ibid.* **162**, 383 (1970).
[78]I. D. Zhongolovich, V. I. Valyaev, A. A. Malkov, and T. B. Sabanina, Trudy ITA AN SSSR, No. 16, 19 (1977).
[79]I. D. Zhongolovich, V. I. Valyaev, and T. B. Sabanina, Pis'ma Astron. Zh. **4**, 38 (1978) [Sov. Astron. Lett. **4**, 20 (1978)].
[80]V. A. Alekseev, B. N. Lipatov, and B. V. Shchekotov, Izv. Vyssh. Uchebn. Zaved. Radiofiz. **19**, 1670 (1976).
[81]A. F. Dravskikh, G. A. Krasinskiǐ, and A. M. Finkel'shteǐn, Pis'ma Astron. Zh. **1**, 43 (1975) [Sov. Astron. Lett. **1**, 21 (1975)].
[82]A. Dravskich, A. Finkelstein, and V. Kreinovich, in: Modern Astrometry, IAU Colloq. No. 48, Vienna, 1979, p. 143.
[83]A. F. Dravskikh, O. M. Kosheleva, V. Ya. Kreǐnovich, and

A. M. Finkel'shteĭn, Pis'ma Astron. Zh. **5**, 422 (1979) [Sov. Phys. Astron. **5**, 227 (1979)].
[84]A. F. Dravskikh, O. M. Kosheleva, V. Ya. Kreĭnovich, and A. M. Finkel'shteĭn, *ibid.* **5**, 300 (1979) [Sov. Astron. Lett. **5**, 160 (1979)].
[85]G. Krasinsky, in: Reference Coordinate System, IAU Colloq. No. 26, Torun, 1976, p. 381.
[86]A. F. Dravskikh and A. M. Finkel'shteĭn, Astrofiz. Issled. **9**, 47 (1977).
[87]A. F. Dravskikh, A. M. Finkelstein, and G. A. Krasinsky, Astrophys. Space Sci. **38**, 255 (1975).
[88]E. P. Fedorov, in: Sistemy koordinat v astrometrii (Systems of Coordinates in Astrometry), Tashkent, 1971, p. 35.
[89]N. D. Umarbaeva, Astron. Zh. **53**, 1132 (1975) [Sov. Astron. **20**, 640 (1976)].
[90]K. I. Kellermann, M. M. Davis, and I. I. K. Pauliny-Toth, Astrophys. J. **170**, L1 (1971).
[91]N. D. Umarbaeva, Soobshch. SAO AN SSSR No. 16, 5 (1976).
[92]N. A. Esepkina, D. V. Korol'kov, and Yu. N. Pariĭskiĭ, Radioteleskopy i radiometry (Radiotelescopes and Radiometers), Nauka, M., 1973, Chap. 9.
[93]H. G. Weiss, Design Studies for 440-foot-diameter Radio Telescope: MIT Technical Report No. 445, 20 Feb. 1968.
[94]Yu. N. Pariĭskiĭ, Abstract of doctoral dissertation, GAO AN SSSR, L., 1970.

Translated by M. V. King